

1 **Variability of mineral dust deposition in the western Mediterranean basin and**
2 **South-East of France**

3
4
5
6
7 Submitted to Atmospheric Chemistry and Physics
8 (ChArMEx Special Issue)
9

10
11 J. Vincent^{1,*}, B. Laurent¹, R. Losno¹⁺, E. Bon Nguyen¹, P. Rouillet², S. Sauvage³, S. Chevaillier¹, P.
12 Coddeville³, N. Ouboulmane¹, A. G. di Sarra⁴, A. Tovar-Sánchez^{5,6}, D. Sferlazzo⁴, A. Massanet⁶, S.
13 Triquet¹, R. Morales Baquero⁷, M. Fornier⁸, C. Coursier⁹, K. Desboeufs¹, F. Dulac¹⁰, G. Bergametti¹
14

15 *Corresponding author: julie.vincent@lisa.u-pec.fr / +33 (0) 145171519
16

17 ¹ Laboratoire Interuniversitaire des Systèmes Atmosphériques (LISA), UMR7583 CNRS, Université
18 Paris 7 Denis Diderot, Université Paris-Est Créteil, Institut Pierre-Simon Laplace, Paris, France

19 ² Ingénierie, Conseil, Assistance technique, Recherche, Etude (ICARE Ingénierie), Paris, France

20 ³ Mines Douai, Département Sciences de l'Atmosphère et Génie de l'Environnement (SAGE), F-59508,
21 Douai, France

22 ⁴ Laboratory for Earth Observations and Analyses (ENEA), Santa Maria di Galeria, Italy

23 ⁵ Andalusian Marine Science Institute (ICMAN, CSIC), Cádiz, Spain

24 ⁶ Institut Mediterrani d'Estudis Avançats (IMEDEA-CSIC/UIB), Balearic Island, Spain

25 ⁷ Departamento Ecologia, Universidad Granada, Granada, Spain

26 ⁸ Mediterranean Institute of Oceanography (MIO), UMR7294 CNRS, UMR235 IRD, Université Aix-
27 Marseille, Université du Sud Toulon-Var, Marseille, France

28 ⁹ Parc national des Ecrins, Le Casset, France

29 ¹⁰ Laboratoire des Sciences du Climat et de l'Environnement (LSCE), UMR 8212 CEA-CNRS-UVSQ,
30 Institut Pierre-Simon Laplace, Gif-sur-Yvette, France

31
32 ⁺ Present address: Institut de Physique du Globe de Paris (IPGP), UMR7154 CNRS, Sorbonne Paris Cité,
33 Université Paris 7 Denis Diderot, Paris, France
34

35 **Abstract**

36

37 Previous studies have provided some insight into the Saharan dust deposition at a few specific locations
38 from observations over long time periods or intensive field campaigns. However, no assessment of the
39 dust deposition temporal variability in connection with its regional spatial distribution has been achieved
40 so far from network observations over more than one year. To investigate dust deposition dynamics at the
41 regional scale, five automatic deposition collectors named CARAGA (“Collecteur Automatique de
42 Retombées Atmosphériques insolubles à Grande Autonomie” in French) have been deployed in the
43 western Mediterranean region during one to three years depending on the station. The sites include, from
44 South to North, Lampedusa Isl., Mallorca Isl., Corsica Isl., Frioul Isl. and Le Casset (South of French
45 Alps). Deposition measurements are performed on a common weekly period at the 5 sites. The mean dust
46 deposition fluxes are higher close to the North African coasts and decrease following a South to North
47 gradient, with values from $7.4 \text{ g m}^{-2} \text{ yr}^{-1}$ in Lampedusa ($35^{\circ}31' \text{N}$ - $12^{\circ}37' \text{E}$) to $1 \text{ g m}^{-2} \text{ yr}^{-1}$ in Le Casset
48 ($44^{\circ}59' \text{N}$ - $6^{\circ}28' \text{E}$). The maximum deposition flux recorded is of $3.2 \text{ g m}^{-2} \text{ wk}^{-1}$ in Mallorca with only 2
49 other events showing more than $1 \text{ g m}^{-2} \text{ wk}^{-1}$ in Lampedusa, and a maximum of $0.5 \text{ g m}^{-2} \text{ wk}^{-1}$ in Corsica.
50 The maximum value of $2.1 \text{ g m}^{-2} \text{ yr}^{-1}$ observed in Corsica in 2013 is much lower than existing records in
51 the area over the 3 previous decades ($11\text{-}14 \text{ g m}^{-2} \text{ yr}^{-1}$). From the 537 available samples, ninety eight
52 major Saharan dust deposition events have been identified in the records between 2011 and 2013.
53 Complementary observations provided by both satellite and air mass trajectories are used to identify the
54 dust provenance areas and the transport pathways from the Sahara to the stations for the studied period.
55 Despite the large size of African dust plumes detected by satellites, more than eighty percent of the major
56 dust deposition events are recorded at only one station, suggesting that the dust provenance, transport, and
57 deposition processes (i.e. wet vs. dry) of dust are different and specific for the different deposition sites in
58 the Mediterranean studied area. The results tend to indicate that wet deposition is the main way of
59 deposition for mineral dust in the western Mediterranean basin, but the contribution of dry deposition (in
60 the sense that no precipitation was detected at the surface) is far to be negligible, and contributes by 10 to
61 46% to the major dust deposition events, depending on the sampling site.

62

63 **1. Introduction**

64

65 A reliable estimation of the dust content in the atmosphere and of its variability in space and time is
66 needed to assess desert dust impacts on the Earth system. The most convenient tools to conduct this
67 assessment are atmospheric dust models in which the atmospheric cycle of mineral dust is represented:
68 dust emissions by wind erosion on arid and semiarid regions; atmospheric transport which is strongly
69 controlled by the meteorological situations; and deposition of dust along their atmospheric path by dry or
70 wet processes. A validation of the closure of the dust budget in atmospheric dust models needs to quantify
71 precisely the amount of emitted dust, the atmospheric dust load, and the dry and wet deposited dust mass
72 (Bergametti and Foret, 2014).

73

74 Significant progress has been made on dust emission modelling during the last two decades (Shao et al.,
75 1993; Marticorena and Bergametti, 1995; Alfaro and Gomes, 2001; Shao, 2004; Marticorena, 2014) and
76 on the dust source monitoring, especially by using satellite observations (Brooks and Legrand, 2000;
77 Prospero et al., 2002; Washington et al., 2003; Schepanski et al., 2012). However, quantitative estimates
78 of dust emissions in atmospheric models are still affected by large uncertainties (Zender et al., 2004;
79 Textor et al., 2006; Huneus et al., 2011), mainly because a direct and quantitative validation of soil dust
80 emissions at a large scale remains not possible. The spatial distribution and temporal variability of
81 atmospheric dust content has also been significantly improved through the development of aerosol
82 products from spaceborne (e.g. Moulin et al., 1997; Torres et al., 2002; Shi and Cressie, 2007; Remer et
83 al., 2008; Nabat et al., 2013), ground-based (Holben et al., 2001) and ship-borne (Smirnov et al., 2011)
84 remote-sensing instruments. Presently, large available datasets of aerosol optical depth (AOD) have been
85 widely and mostly used to validate dust atmospheric contents simulated by 3D models at global (e.g. Chin
86 et al., 2002; Ginoux and Torres, 2003; Huneus et al., 2011) or regional scales (e.g. Cautenet et al., 2000).

87

88 Atmospheric dust particles are removed from the atmosphere by dry and wet depositions processes (Duce
89 et al., 1991; Schulz et al., 2012). These two sinks, which counterbalance dust emissions on the global
90 scale, control the atmospheric lifetime of dust particles (Bergametti and Fôret, 2014). However, rather
91 little attention has been paid to dust deposition and few experiments were dedicated to test dust deposition
92 schemes against in situ data. There is an urgent need for further research and measurements of dust
93 deposition. Dust models are mainly validated against proxies for the atmospheric dust load, e.g. AOD,
94 concentrations, dust vertical profiles, or combinations of these. However, at least two of the terms
95 emission, dust load and deposition need to be documented to close the dust mass budget.

96

97 In this paper, we will present the results over a three-year period concerning atmospheric mass deposition
98 measurements associated with Saharan dust transport over the Western Mediterranean Basin. The main

99 goal of the sampling strategy is to provide data that can be used directly to test the dust mass budget in
100 dust transport model. This data set of Saharan dust deposition in the Western Mediterranean region can
101 also be used to identify the transport patterns and the provenance of the dust. To do that, deposition
102 measurements are coupled with satellite observations and air-mass trajectories.

103

104

105

106 **2. Deposition measurement in the Mediterranean region**

107

108 Atmospheric deposition fluxes have been measured in the Mediterranean region during the last fifty
109 years. Table 1 gathers the direct deposition measurements performed both close to Saharan dust source
110 areas and far away on both sides of the Mediterranean basin. Most of these deposition mass fluxes were
111 obtained directly by weighting the deposited mass, the others being derived from aluminum deposition
112 measurements assuming that this element contributes for about 7 to 8% of the total dust mass
113 (e.g. Guieu et al., 2002). Note that dust deposition can be also estimated indirectly based on the
114 measurements of atmospheric aerosol concentrations and assuming dust dry deposition velocity and
115 scavenging ratio (e.g. Le Bolloch et al., 1996).

116

117 Dust deposition measurements close to the North African dust sources are rare: dust deposition fluxes
118 were only measured in Morocco, Tunisia and Libya. The deposition samples from Tunisia and Morocco
119 (Guieu et al., 2010) were collected at sampling sites located along the Mediterranean coasts and indicate
120 deposition fluxes ranging from 7 to 23 g m⁻² y⁻¹. Dust deposition sampled in Libya (O'Hara et al., 2006),
121 in 24 stations located from the North to the South of the country, provide significantly higher deposition
122 fluxes, ranging from 40 g m⁻² yr⁻¹ to 420 g m⁻² yr⁻¹.

123

124 In the Mediterranean basin itself, dust deposition fluxes exhibit a large spatial variability ranging over
125 more than one order of magnitude, from 2 g m⁻² yr⁻¹ to more than 27 g m⁻² yr⁻¹ in the western basin and
126 from 4 g m⁻² yr⁻¹ to ~100 g m⁻² yr⁻¹ in the eastern basin (Table 1), but also a strong inter-annual variability
127 with fluxes ranging from 4 to 26 g m⁻² yr⁻¹ in Corsica over an 11-year period (Loÿe-Pilot and Martin,
128 1996). It must be emphasized that most of the temporal variability at a given site is due to the occurrence
129 of very intense but rare events with fluxes of several g m⁻² that dominate the annual deposition flux when
130 they occur (see for instance Bergametti et al., 1989; Loÿe-Pilot et al., 1996; Fiol et al., 2005).

131

132 These measurements provide a picture of the dust deposition in the Mediterranean basin, the
133 heterogeneity of data does not allow to precisely investigate the spatial and temporal variabilities of the
134 dust deposition fluxes. Indeed, most of these dust deposition measurements were performed either in one

135 site during a long time period (e.g. datasets obtained in Corsica between 1984 and 1994 by Lojze-Pilot
136 and Martin, 1996, or in Crete between 1988 and 1994 by Pye, 1992 and Mattson and Nihlén, 1994), or on
137 a network of several stations but during a much shorter time period. Moreover, the dust deposition fluxes
138 were generally not measured with the same devices. This complicates the comparison of the data
139 collected at the different sites.

140

141 Thus, a better understanding of the dust deposition in the Mediterranean basin, and especially of its
142 spatial and temporal variability, requires measurements performed simultaneously on at several stations
143 and with similar devices during a long-time period. With this objective, a new deposition sampler was
144 developed for use at remote sites in full autonomy over several months (Laurent et al., 2015).

145

146

147

148 **3. Materials and methods**

149

150

151 **3.1 The CARAGA deposition collector**

152

153 In order to be able to maintain over a long time period a network to measure dust mass deposition fluxes,
154 our strategy was to sample only the insoluble deposition. This simplifies a lot the design of the collector
155 and the on-site operations. More than 80% of the total Saharan dust deposition mass in the Mediterranean
156 basin occurs in the form of insoluble material (Guerzoni et al., 1993; Avila et al., 2007). As a
157 consequence, an automatic collector called CARAGA (“Collecteur Automatique de Retombées
158 Atmosphériques insolubles à Grande Autonomie”) was developed in collaboration between the ICARE
159 Ingénierie Company and the Laboratoire Interuniversitaire des Systèmes Atmosphériques (Figure 1). The
160 CARAGA was designed to require limited human interventions and to be produced in small series to
161 develop a standardized deposition network in remote areas (Laurent et al., 2015). A collecting open
162 funnel (0.2 m²), fixed on a steel structure at least 2.5 m above ground level (agl), allows the collection of
163 both dry and wet deposition. The funnel vibrates and is rinsed automatically with pure water at the end of
164 a sampling time period to drive down the collected particles on a filter. The online passive filtrating
165 system allows collecting the particles on one of the filters which are installed in a motorized rotating unit
166 carrying 25 filter holders. A solar panel insures the power supply of the CARAGA. A new filter is set
167 automatically in the sampling position for each sampling step whose duration can be defined through an
168 electronic interface. The funnel vibration and rinsing can be programmed to operate two times before
169 every filter change. The CARAGA system is best suited for the collection of the non-soluble fraction of
170 dust, but it could be used for evaluating other inorganic or organic particles after adapting the sampling

171 and lab protocols. A complete description of the CARAGA collector can be found in Laurent et al.
172 (2015).

173

174

175 **3.2 Implementation of the deposition network**

176

177 The deposition network in the western Mediterranean basin is constituted of five CARAGA instruments
178 installed mainly on Mediterranean island coasts (Figure 2). This network is thought to allow dust
179 deposition sampling along a South-to-North transect, from near the North African coast to the South-East
180 of France, covering about 1050 km from South to North and 870 km from West to East. The network is
181 constituted of four island sites and one continental site. The first CARAGA was installed in October 2010
182 on the small elongated Pomègues Island which is part of Frioul Islands, a 2-km² archipelago. The Frioul's
183 site is sited in the Gulf of Lion a few km of Marseille under the influence of natural and anthropogenic air
184 masses. The sampler is at ~45 m in altitude on the small ridge that crosses the whole island, distant from
185 the sea by less than 150 m on two opposite sides. This site, is also a site of the French Mediterranean
186 Ocean Observing System for the Environment (MOOSE; <http://www.moose-network.fr/>) instrumented by
187 the Mediterranean Institute of Oceanography. In July 2011, a second collector was installed at Le Casset
188 in the southern French Alps, at ~1850 m in altitude. This site is one of the 13 sites of the network MERA
189 (Observatoire National de Mesure et d'Evaluation en Zone Rurale de la Pollution Atmosphérique à
190 Longue Distance, <http://ce.mines-douai.fr/pages/observatoire-mera/>) by belonging to EMEP (European
191 Monitoring and Evaluation Program, EMEP; <http://www.emep.int/>). CARAGA samplers were afterward
192 installed: (i) at 7 m in altitude and ~70 m from the sea shore at the Ses Salines lighthouse site on the
193 southeastern tip of Mallorca Island (http://imedea.uib-csic.es/icg/Faro/home_en/), a research site operated
194 by the Institut Mediterrani d'Estudis Avançats (IMEDEA), in July 2011; and (ii) at 38 m in altitude and
195 ~20 m of the border of the cliff of the northwestern coast of Lampedusa Island located in central
196 Mediterranean, at the Global Atmosphere Watch (GAW) regional background station
197 (<http://www.lampedusa.enea.it/>) operated by the Laboratory for Earth Observations and Analyses of the
198 Agenzia Nazionale per le Nuove Tecnologie, l'Energia e lo Sviluppo Economico Sostenibile (ENEA;
199 supersite of the Chemistry-Aerosol Mediterranean Experiment, ChArMEx, (<http://charmex.lsce.ipsl.fr>) in
200 September 2011. The last CARAGA was installed at 75 m in altitude and ~300 m from the sea shore on
201 the northern tip of Cape Corsica, headland of Corsica Island. It is close to the AERONET sunphotometer
202 station downhill the French Navy semaphore of Ersa and a few km from the Ersa supersite of the
203 ChArMEx program. At the stations, the precipitation amounts are available at least on a daily basis.

204

205

206 **3.3 Sampling and lab protocol**

207

208 Atmospheric total (wet + dry) insoluble deposition is collected at the five sampling sites over the period
209 2011-2013. For this study, a one-week sampling duration was chosen as a compromise between
210 maximizing the opportunity of sampling single dust plume deposition event and a long autonomy of the
211 collector, i.e. up to 25 sampling weeks. The same sampling duration is programmed at the 5 sites, with an
212 automatic change of the filter every Thursday at 12:00 UTC. 537 weekly atmospheric deposition samples
213 were collected. At least one year of continuous deposition measurements is available from every station,
214 the longest time series being from the Frioul site (January 2011 to December 2013). Depending on the
215 site, the data recovery rate of weekly atmospheric deposition samples ranges from 77% to 91% for the
216 sampling period and at least 1-yr of continuous measurements is available for each station.

217

218 Atmospheric particulate concentrations measured in the Mediterranean suggest that more than 90% of
219 dust particles mass is in the coarse mode (diameter larger than 1.2 μm aerodynamic diameter) (Sciare et
220 al., 2005). Thus, after flow speed tests, we choose to use the AA Millipore cellulose ester filter with a 0.8
221 μm porosity. Moreover, Sheldon (1972) indicated that Millipore cellulose ester filters, with a porosity
222 ranging from 0.45 to 8 μm , have high percentages of retention of particles of 1 μm ranging from 80 to 100
223 %. Prospero (1999) collected atmospheric particles on filters which were placed in a muffle furnace
224 during 14h at 500°C, the ash residue weigh being assumed to be mineral dust. To determine the mineral
225 mass collected on the filters an ignition and weighing protocol was defined and presented in Laurent et al.
226 (2015). Briefly, it is based on the ignition of the sampled filters following a progressive increase in
227 temperature up to 550°C to remove organics and carbon by oxidation. Thus, the material remaining in the
228 ashes is mineral matter. This mineral mass is then determined by a weighing procedure in controlled
229 conditions. This protocol insures a good repeatability and reliability ($\pm 10^{-3}$ g by filter) in the
230 determination of the mineral masses, limiting the loss of particles during filter handling (especially for
231 filters highly loaded with dust particles). Moreover, if small insects, vegetal debris, pollens or other
232 organic matters are collected on the filters, they are manually removed only if this manipulation does not
233 affect the sample. If the removal of these elements could damage the sample, we leave them on the filter
234 considering that samples ignition eliminates the organic matter (Laurent et al., 2015).

235

236 **3.4 Air mass trajectories and satellite observations**

237

238 Air-mass trajectories and satellite observations can be jointly analysed to point out the provenance of the
239 dust deposition measured at the stations.

240

241 Air-masses trajectories computed using the HYSPLIT model (Draxler et al., 2003;
242 <https://ready.arl.noaa.gov/HYSPLIT.php>) are commonly used to trace the origin of the air masses

243 transporting mineral dust (Escudero et al., 2011; Meloni et al., 2008) or atmospheric pollutants (Jorba et
244 al., 2004; Pongkiatkul and Kim Oanh, 2007). The statistical analysis of numerous backward trajectories
245 from receptor sites has turned out to be a valuable tool to identify sources of atmospheric trace substances
246 (Stohl, 1998; Scheifinger and Kaiser, 2007).

247

248 Since the transport of Saharan air masses towards the western Mediterranean basin can occur at various
249 altitudes in the troposphere (Bergametti et al., 1989; Martin et al. 1990; Hamonou et al., 1999; di Sarra et
250 al., 2001 ; Israelevich et al., 2002 ; Meloni et al., 2008; di Iorio et al, 2009), 4 days backward air masses
251 trajectories starting every day at 12:00 UTC were computed starting at 0, 500, 2000, 3000, 4000 and
252 5000 m agl for each of the five sampling stations. When the circulation of the model air masses is too slow
253 over the western Mediterranean basin, the duration of the backward trajectories was extended to 6 days.

254

255 These air-mass trajectories were combined with Aerosol Optical Depth (AOD) products of the Moderate
256 Imaging Spectrometer (MODIS, <http://modis.gsfc.nasa.gov/>) to identify, as best as possible, the
257 provenance of the Saharan dust plume. The daily MODIS deep blue AOD at 550 nm over land and
258 MODIS AOD at 550 nm over the oceanic surfaces (Levy et al., 2013) were used. When MODIS AOD
259 was unavailable due to cloud cover, we also examined the EUMETSAT MSG/SEVIRI dust false-colour
260 composite product available from ICARE Geo Browse Interface (<http://www.icare.univ-lille1.fr/>), which
261 gives the opportunity to follow the transport of the dust plume every 15 min (e.g. Schepanski et al.,
262 2007).

263

264 Once the dust provenance identified, the HYSPLIT model was also used to compute forward air mass
265 trajectories in ensemble mode (i.e., multiple trajectories from the selected starting location by offsetting
266 the meteorological data) or in matrix mode (i.e., starting from the borders of these identified dust
267 sources). These forward air mass trajectories at 00:00 and 12:00 UTC were computed starting from the
268 dust provenance area at an altitude of 500 m agl which can be considered as a common dust entrainment
269 altitude (Meloni et al., 2008). We checked the coherence between the backward and forward air mass
270 trajectories computed for studied dust cases. We also checked for each forward trajectory the altitude of
271 the air-mass and if precipitation occurred during transport.

272

273

274

275 **4. Results and discussion**

276

277

278 **4.1 Weekly mineral dust deposition in the western Mediterranean basin**

280 The weekly fluxes of insoluble mineral deposition measured at the 5 sites are reported in Figure 3. The
281 highest weekly deposition fluxes are recorded at the two stations nearest to the Sahara desert: 3.2 g m^{-2}
282 wk^{-1} and $2.7 \text{ g m}^{-2} \text{ wk}^{-1}$ were measured at Mallorca and Lampedusa. The maximum deposition recorded
283 for the stations located in the north-western Mediterranean basin and South of France (Corsica, Frioul and
284 Le Casset) is almost one order of magnitude lower (0.53 , 0.34 and $0.17 \text{ g m}^{-2} \text{ wk}^{-1}$, respectively). The
285 same trend is observed when considering the deposition fluxes cumulated over a 1-year period without
286 sampling discontinuities. In fact, the highest annual deposition fluxes are: $7.4 \text{ g m}^{-2} \text{ yr}^{-1}$ in Lampedusa for
287 2012; $5.8 \text{ g m}^{-2} \text{ yr}^{-1}$ in Mallorca for 2013; $2.1 \text{ g m}^{-2} \text{ yr}^{-1}$ in Corsica for 2013; $3.5 \text{ g m}^{-2} \text{ yr}^{-1}$ in Frioul for
288 2012; and $0.9 \text{ g m}^{-2} \text{ yr}^{-1}$ in Le Casset for 2012. Thus, a South-to-North decreasing gradient in the intensity
289 of the mineral dust deposition is observed over the western Mediterranean basin with a flux about 2 to 8
290 times lower in the northern part of the basin and southern France than in the southern basin. Previous
291 observations **also** pointed out a gradient of dust content in the western Mediterranean atmosphere (see for
292 example Barnaba and Gobbi, 2004; Pey et al., 2013).

293

294 In the late 1980s and 2000s, the mean annual Saharan dust deposition measured in Corsica by Loÿe-Pilot
295 et al. (1986), Loÿe-Pilot and Martin, (1996) and TERNON et al. (2010) were of 14.0 , 12.5 and 11.4
296 $\text{g m}^{-2} \text{ yr}^{-1}$, respectively. Bergametti et al., (1989) also measured a mean annual deposition of 11.0
297 $\text{g m}^{-2} \text{ yr}^{-1}$ in Corsica. These deposition fluxes are significantly higher than the one we measured at the
298 Corsica station from January to December 2013. These studies also point out a high inter-annual
299 variability of the atmospheric deposition in the western Mediterranean basin. Investigating 11 years of
300 atmospheric deposition in Corsica, Loÿe-Pilot and Martin (1996) reported deposition fluxes ranging from
301 4 to $26.2 \text{ g m}^{-2} \text{ yr}^{-1}$. These authors indicate that no deposition event greater than 1 g m^{-2} was recorded in
302 the years for which the annual atmospheric deposition was low in Corsica, suggesting that the interannual
303 variability of dust deposition in Corsica was driven by the annual occurrence of very intense Saharan dust
304 deposition events. The contribution of such dust pulses to the annual atmospheric deposition flux in the
305 western Mediterranean has been underlined many times in the literature. For example, Bergametti et al.,
306 (1989) reported that a deposition event of only 3-days occurring in March 1986 has contributed for more
307 than 30% of the annual atmospheric deposition measured in Corsica for elements such as Al or Si.
308 Guerzoni et al., (1997) also mentioned that a single Saharan dust outbreak can account for 40-80% of the
309 annual deposition flux. In February 2004, TERNON et al. (2010) measured an extreme case of dust
310 deposition in the Ligurian sea area (22 g m^{-2} for two weeks). This Saharan dust event represented almost
311 90% of the Saharan inputs reported for 2004 at the Cap Ferrat site (TERNON et al., 2010).

312

313 The annual deposition flux we measured in Corsica corresponds to a low dust deposition year. This is also
314 supported by the fact that none of the weekly deposition fluxes we measured exceeds 1 g m^{-2} , the higher

315 deposition flux measured in Corsica being $0.53 \text{ g m}^{-2} \text{ wk}^{-1}$. However, compared to previous deposition
316 measured in Corsica, even the annual deposition fluxes measured at the southern stations of the western
317 Mediterranean basin (Lampedusa and Mallorca) are lower, suggesting that the years 2011, 2012 and 2013
318 probably correspond to a low atmospheric deposition period. This observation is in agreement with the
319 analysis performed by Pey et al. (2013) from PM10 measurements performed in the Mediterranean region
320 over the period 2001-2011 which concluded to a decrease of the contribution of Saharan dust events to
321 the PM10 load. As mentioned by these authors and according to the study of Moulin et al. (1997), this
322 decrease in the Saharan dust transport over the western Mediterranean Sea is probably due to the
323 continuous decrease of the North Atlantic Oscillation (NAO) index in winter during the period 1990-2012
324 and in summer since 2006.

325 326 327 **4.2 Selection of the most intense weekly deposition fluxes**

328
329 The previous studies mentioned above indicated that the largest deposition events observed in the western
330 Mediterranean basin are strongly associated with Saharan dust transports (Bergametti et al., 1989; Lojé-
331 Pilot and Martin, 1996; Guerzoni et al., 1999). We decided to give a particular attention to the most
332 intense weekly deposition flux (MID) measured at each station and to verify if these high deposition
333 events were linked to Saharan dust transport towards the Mediterranean Sea. We cannot exclude that local
334 mineral contribution, especially during high wind speed periods at the station, may affect some samples,
335 in particular those for which the deposition due to long-range transported dust is the lowest. Moreover,
336 for the station located the farthest from the African coasts such as Frioul or Le Casset, the anthropogenic
337 background in refractive material may also contribute for a limited part to the insoluble mineral
338 deposition. Among the MID, the most intense Saharan dust deposition samples (MIDD) and the
339 corresponding dust deposition events (DDE) will be discussed.

340
341 To select the MID, we first merged all the weekly samples collected at the different stations (537
342 samples) and then selected the weekly deposition greater than the last sextile of the dataset, i.e. the
343 16.67% highest deposition values (i.e. 90 samples). This leads to a threshold weekly deposition flux of
344 $9.3 \cdot 10^{-2} \text{ g m}^{-2} \text{ wk}^{-1}$. The 90 highest deposition values were thus retained by using this threshold,
345 independently of the station where they have been measured. However, as shown before, the intensity of
346 the atmospheric deposition is higher at the stations located the nearest to the North African dust source
347 areas. This means that even a relatively high deposition event occurring in the northern part of the basin
348 may be excluded from the selection because its deposition flux is lower than the overall threshold value.
349 To correct this bias, we added a second criterion which consists in also retaining, for a given station, all
350 the samples for which the weekly deposition flux is greater than the geometric mean (m_g) plus the

351 geometric standard deviation (σ_g) calculated for each station, i.e. $m_g * \sigma_g$, statistical tests having shown
352 that the deposition fluxes measured at each station fitted either a log-normal or a Gamma distribution
353 (values below 10^{-4} g for a sample were assumed to be equal to this weighing detection limit). This second
354 criterion allows the minimum selection of the upper sextile of a lognormal distribution. It leads to select
355 18 additional samples at the 2 stations where the average fluxes are the lowest: 4 more samples from
356 Corsica (fluxes >0.050 g m⁻² wk⁻¹) and 14 from Le Casset (>0.036 g m⁻² wk⁻¹). Table 2 reports the 108
357 MID distribution by station, 54% of them having been sampled in the southern stations of Lampedusa and
358 Mallorca. The MID represent at least more than half of the whole deposition flux measured at each station
359 (Table 2).

360

361 The MID events being selected, we verified whether these deposition events were or nor associated with
362 air-masses originating from the Saharan desert. To point out the provenances and the main transport
363 pathways of deposition events at each station, HYSPLIT air-mass trajectories and satellite aerosol
364 observations were jointly analyzed as presented in section 3.4. Among the 108 MID samples, only one
365 sample collected at Le Casset was not associated with at least one air mass trajectory having crossed
366 Northern Africa during the sampling week.

367

368 For each MID, we identified by using MODIS AOD or MSG satellite observation where dust is coming
369 from. Figure 4 illustrates the different satellite observations and air mass trajectories used to identify the
370 dust provenance area and transport pattern associated with dust deposition in the western Mediterranean
371 basin. 98 samples among the 107 MID present an air mass coming from North African areas with high
372 AOD and reaching the stations. Hereafter, these 98 most intense Saharan dust deposition samples are
373 called MIDD. For the remaining 9 cases, the absence of matching between high AOD observed from
374 satellite images and air mass trajectories linking the dust provenance region to the sampling stations does
375 not necessary mean that these cases are not cases of Saharan dust deposition. The MIDD accounts for
376 84%, 78% and 73% of the deposition in Lampedusa, Mallorca and Corsica, respectively, while it
377 contributes for around 50% in Frioul and Le Casset (Table 2).

378

379

380 **4.3 Seasonality of the most intense dust deposition (MIDD)**

381

382 To look at the seasonality of the MIDD occurrence for the studied period, the fact that each month of the
383 year has not been sampled with the same frequency at each sampling station has to be taken into account.
384 We computed the number of weeks which have been sampled for each month and for each station. A
385 weighting coefficient $a_{(M)}$ was computed for each station by dividing the number of sampled weeks for

386 each month (M) by the total number of weeks of sampling at each station. $F_{(M)}$, the weighted number of
387 MIDD occurrences for a given per month M was then computed as:

$$F_{(M)} = \frac{N_{(M)}}{a_{(M)}} \quad (\text{Eq. 1})$$

388 where $N_{(M)}$ is the number of MIDD during a given month.

389 Figure 5 reports the number of MIDD occurrence per month at each site. Most of the MIDD occurred
390 during spring (March-June): 53% in Le Casset, 49% in Frioul, 81% in Corsica, 38% in Mallorca and 55%
391 in Lampedusa. A second maximum is observed in autumn in Mallorca and Lampedusa, and at the end of
392 summer and early autumn in Frioul, Corsica and Le Casset. From their long-term data set in Corsica,
393 Loÿe-Pilot and Martin (1996) also observed the most frequent and intense dust events in spring and
394 autumn. According to Bergametti et al. (1989), the frequency of Saharan inputs in Corsica seems to be the
395 highest during spring and summer, 80% of the events being observed between March and October 1985.
396 TERNON et al. (2010) observed high deposition in spring and summer with a maximum in June from their
397 measurements performed in the Ligurian area between 2003 and 2007. Avila et al. (1997) showed that the
398 occurrence of red rain episodes in northeastern Spain between 1983 and 1994 were higher in autumn and
399 spring. The dust deposition seasonality cannot be directly compared with other atmospheric observations.
400 For instance in Lampedusa, the seasonality of atmospheric dust content and dust deposition are different.
401 Maximum AOD indicate highest dust atmospheric content in summer in 2001-2005 (Meloni et al., 2004;
402 2008) while the crustal aerosol contribution to PM10 measurements performed between 2004 and 2010
403 does not show any evident seasonal pattern. Marconi et al. (2014) mentioned that in Lampedusa no
404 significant correlation between aerosol optical thickness and PM10 or non-sea-salt Ca is found for the
405 period June 2004-December 2010. These authors suggested that even when the dust is very likely present
406 in the lower and mid-troposphere simultaneously, the aerosols observations at the surface are generally
407 decoupled from what takes place above in the atmospheric column.

408

409 Our results point out that the stations of the network are not systematically concerned by dust deposition
410 at the same period. To fully understand the variability of Saharan dust deposition in the western
411 Mediterranean basin, several sampling sites are required to perform direct deposition measurements.

412

413

414 **4.4 Identification of Saharan dust deposition events**

415

416 The number of stations operating when a MIDD was recorded is given in Table 3. 98 MIDD have been
417 collected during 75 different weeks of sampling and 82% of these MIDD were recorded when at least 4
418 stations were simultaneously operating. However, only 17 of these MIDD have affected more than 1

419 station during the same sampling week (12 at 2 stations, 4 at 3 stations, and 1 at 4 stations). 75% of the
420 cases when at least 2 stations recorded a MIDD associated the Mallorca stations or the Lampedusa station
421 with northern stations. Only 2 cases associated at least both Lampedusa and Mallorca stations. The
422 stations the most often associated to a given MIDD are (i) Frioul and le Casset (6 cases for which at least
423 these 2 stations are associated), (ii) Mallorca and Corsica (5 cases for which at least these 2 stations are
424 associated). This suggests that, in the western Mediterranean basin, the MIDD are associated with
425 different dust provenance and transport pathways, and/or the dust plumes are washed out by precipitation
426 during their transport over the basin.

427

428 The joint analysis of the HYSPLIT air mass trajectories and MODIS AOD allows us to identify where
429 dust deposited at the stations for the MIDD is likely coming from. During a sampling week, several dust
430 deposition events (DDE) can be identified and contribute to the weekly deposition flux. A dust event
431 contributing to dust deposition during several days at a station is considered as a single DDE. A MIDD
432 can be a combination of several DDE originating from different dust areas. We identified 132 DDE for
433 the studied period: 50 reached Lampedusa, 27 Mallorca, 22 Frioul, 15 Corsica and 18 Le Casset. The
434 number of events contributing to the dust deposition is greater for the stations close to the North African
435 dust sources.

436

437 For each DDE, the localization of the highest AOD southernmost along the modelled air mass trajectory
438 defined a rough region where dust comes from. As mentioned by Meloni et al. (2008), due to the low
439 resolution of the model meteorological fields and transport model intrinsic errors, the dust location can be
440 relatively wide. It should also be kept in mind that other sources located along the pathway of the dust
441 plume can also contributed to the dust uplifts. Thus, we defined 7 large dust provenance areas (DPA) by
442 grouping together the closest dust localizations (Figure 6): Niger and Chad (DPA1), northern Mali and
443 southern Mauritania (DPA2), Western Sahara and South Morocco (DPA3), Central Algeria (DPA4),
444 Libya (DPA5), Tunisia and East Algeria (DPA6), and North Morocco and north-western Algeria (DPA7).

445

446 The number of DDE at each station (weighted as in §3.3 and expressed in %) originating from the 7 areas
447 are reported in Figure 6. 73% of DDE in Frioul and 69% of DDE in Le Casset come from the western part
448 of the Sahara (DPA2, 3 and 7). The Western Sahara (DPA3) and Tunisia (DPA6) are the most frequent
449 provenance of DDE reaching Mallorca. Dust deposited during the DDE in Lampedusa generally come
450 from the Tunisian (DPA6) and Libyan (DPA5) regions and the Central Algeria (DPA4). DDE in Corsica
451 generally come from the Western Sahara and South Morocco (DPA3), Tunisia and East Algeria (DPA6)
452 and Libya (DPA5), and the same level of similarity can be observed between the dust provenance areas
453 affecting Mallorca and Corsica than between Corsica and Lampedusa. We also noted that provenance
454 areas, even south of 20°N, like Niger and Chad (DPA1), and northern Mali and southern Mauritania

455 (DPA2), could contribute to DDE (DPA1 for Frioul and Lampedusa, DPA2 for all the stations). Tunisian
456 and Libyan sources have been pointed by Salvador et al. (2014) for specific dust outbreak observed in
457 spring in Balearic Islands and central Mediterranean. This dust transport pathway can be due to high
458 pressure systems located over these sources (Salvador et al., 2014). Moreover, Marconi et al. (2014) also
459 pointed out source regions located in Tunisia-Algeria and Libya to explain atmospheric dust content in
460 Lampedusa. Meloni et al. (2008) indicated the Morocco, Algeria and Tunisia as dust loading areas, as
461 well as southern areas in Mauritania-Mali.

462

463 These results confirm that the different parts of the western Mediterranean basin are not affected in the
464 same proportion by Saharan dust coming from different regions. It is nevertheless important to keep in
465 mind that what was tracked here is the southernmost occurrence of dust along the trajectory associated to
466 intense dust deposition events. Hamonou et al. (1999) have shown that dust layers of different origins can
467 also be present concurrently over a given station in the northern part of the Mediterranean.

468

469

470 **4.5 Transport routes of the Saharan dust deposition events**

471

472 The main transport routes associated with the 132 DDE in the western Mediterranean Sea were
473 investigated. We classified the forward air mass trajectories computed for each DDE depending on their
474 pathway. The six most frequent types of trajectories (representing 96.3% of all trajectories) are illustrated
475 in Figure 7. Note that 4 cases among them were classified as “others”, each of them corresponding to a
476 trajectory observed only one time during the studied period. The air-mass trajectories over the western
477 Mediterranean basin are often transported in high altitude (Escudero et al., 2005; Querol et al., 2009).
478 Low level transport of dust are mostly observed at Lampedusa. Trajectories types (a), (c) and (d) are the
479 most frequent transport ways of Saharan dust towards the western Mediterranean basin, since they all
480 together account for almost 70% of all trajectories. Trajectories type (a) correspond to a straight transport
481 of dust emitted from sources located in Tunisia and/or Libya towards Lampedusa and the the eastern part
482 of western Mediterranean basin. This type of trajectory is the dominant transport in spring (Figure 8).
483 Trajectories type (c) correspond to transport from sources located in West Algeria/Morocco and
484 Mauritania/Mali towards the western part of the basin and type (d) to transport in a West to East flow
485 from sources located in western and central Sahara and mainly towards the southwestern Mediterranean
486 Basin. They are the dominant Saharan dust transport pathways during summer (Figure 8). These
487 trajectories have already been mentioned in previous studies as major transport ways for Saharan dust
488 over the Mediterranean Sea (Bergametti et al., 1989; Guerzoni et al., 1997; Moulin et al., 1998;
489 Israelevich, 2003; Meloni et al., 2008; Marconi et al., 2014). Even if they are less frequent, Saharan dust
490 transport trajectories of type (b) (straight transport towards the westernmost part of the Mediterranean

491 basin from sources located in North Morocco and West Algeria) and (e) (stagnant air masses and cyclonic
492 flow centered over the Atlas and southern Mediterranean) represent 12.1% and 10.6% of all trajectories,
493 and often occur in spring (Figure 8).

494

495 HYSPLIT model trajectories and precipitation were used to examine whether the different transport
496 trajectories to the western Mediterranean Basin were systematically associated or not with precipitation
497 during transport. We consider a trajectory with an occurrence of precipitation along its path between the
498 Saharan dust provenance area and a given station as a “wet transport case”, whatever the rainfall rate.
499 Main uncertainties are due to the low spatial resolution of the meteorological data set which prevents, for
500 example, accounting for the summer precipitation due to convective cells (Meloni et al., 2008). Moreover,
501 the precipitation is precipitation rate at the grid cell where the trajectory is located and does not take into
502 account the air mass altitude transport. Figure 9 presents the proportion of Saharan dust trajectories
503 coming from each dust provenance area (identified in §3.4) and for which precipitation during transport
504 have been computed by the HYSPLIT model. Dust air masses from the western Sahara have the highest
505 probability (> 60%) to be washed during transport. On the opposite, dust air masses from southern and
506 central Sahara are transported about 2/3 of the time in dry conditions. This suggests a more efficient
507 transport of dust from these Saharan regions to the western Mediterranean basin. Air masses coming from
508 the most eastern source regions exhibits intermediate values, with a 50% probability to be washed during
509 transport.

510

511 Results on dust provenance and transport pathways of the DDE suggest that different parts of the western
512 Mediterranean basin are affected by dust deposition events at different periods and from different dust
513 source regions. Dust masses follow different transport trajectories to reach the Mediterranean, some of
514 them being probably washed by precipitation during their transport. This means that Saharan dust inputs
515 to the different parts of the western Mediterranean Basin do not occur at the same time, and can differ in
516 intensity and in composition.

517

518

519 **4.6 Dry and wet deposition**

520

521 In this study, no direct measurements of dry-only and wet-only deposition are performed. However, in
522 order to provide information on the relative importance of dry and wet deposition to the MIDD, the daily
523 precipitation measured were analyzed in combination with forward dust air mass trajectories starting from
524 the identified provenance areas and reaching the sampling sites. When no precipitation is recorded we
525 consider that dust deposition is driven by dry deposition processes. As mentioned by Löye-Pilot and
526 Martin (1996), significant deposits can occur in almost “dry conditions”, i.e. very low and short rain

527 events and/or fog periods that classical meteorological rain gauges cannot detect. As a consequence, in
528 these cases, the deposition is considered as dry and this leads to a possible overestimation of the
529 contribution of the dry-only deposition to the total deposited flux. The air mass trajectories provide for
530 each identified dust event a theoretical date of its arrival at a given sampling station. As mentioned above,
531 there are uncertainties on the computed trajectories due to both the model and the resolution of the
532 meteorological fields. Moreover, in most cases, the starting date of the trajectory from the source regions
533 (as determined by looking at the satellite images) is known with a precision not better than +/- 12h. Thus,
534 a dust deposition event for which no precipitation is recorded at the station 24 h before and up to 72 h
535 after the dust plume arrival is defined as “dry”. The 72-h time period after the arrival of the dust air mass
536 over the sampling site is splitted in three periods (24, 48 and 72 h) in order to take into account for the
537 duration of the dust events that can last more than one day (Table 4). For each of the 98 MIDD, the
538 numbers of dry, wet and mixed (wet + dry) DDE were computed. Obviously, this procedure
539 underestimates the number of dry only deposition cases and provides only a lower estimate of dust dry
540 DDE events relatively to the total DDE identified at each station.

541

542 Table 4 reports, for each sampling station, estimated proportions of the wet-only, dry-only, and mixed
543 DDE to MIDD (in terms of occurrences and mass fluxes). Between 36% and 82% of MIDD (depending
544 on the sampling stations) occur in only wet conditions. The deposition in the northern stations is
545 dominated by wet deposition (77% to 82% of the total mass deposition in Le Casset, 61% to 66% in
546 Frioul, 69% to 74% in Corsica). For the southern stations, Lampedusa and Mallorca, wet deposition could
547 contribute to 51% and 36% to 41% of total deposition mass, respectively. Even if the wet or dry
548 deposition events can be roughly classified following our approach, the occurrence and the intensity of
549 dry deposition events are far to be negligible. In terms of mass, dry deposition represents between 10%
550 and 46% of the deposited mass, the lower contribution being observed in the remote island sites of
551 Mallorca (10% to 15%) and Corsica (10% to 15%). The highest MIDD measured in Lampedusa ($2.7 \text{ g m}^{-2} \text{ wk}^{-1}$;
552 20% of the total deposition flux, respectively) corresponds to a single wet deposition DDE.
553 However, the second highest MIDD measured in Lampedusa ($2.1 \text{ g m}^{-2} \text{ wk}^{-1}$; 16% of the total deposition
554 flux) corresponds to 2 successive dry DDE. In this latter case, dust plumes were transported below
555 2000 m. Such a low altitude dust transport in this area was also reported by Barnaba and Gobbi (2004).
556 The highest MIDD measured in Mallorca at the end of April 2013 ($3.2 \text{ g m}^{-2} \text{ wk}^{-1}$; 42% of the total
557 deposition flux) resulted from 3 DDE (1 dry and 2 wet). For the studied period, our results shows that the
558 most intense dust deposition fluxes can be due to single or several successive DDE and can involve wet
559 deposition as well as dry deposition events.

560

561

562

563 5. Conclusion

564

565 A network of 5 sampling sites was deployed from 2011 on the western Mediterranean region to measure
566 the insoluble atmospheric deposition fluxes. It included from South to North an Italian site (Lampedusa
567 Isl.), a Spanish site (Mallorca Isl.) and 3 French sites (Corsica Isl., Frioul Isl., and Le Casset in
568 southeastern France). The data recovery rate varied between 77% and 91% depending on the station. The
569 deposition dataset acquired between 2011 and 2013 include 537 weekly samples. It allowed us to
570 investigate Saharan dust deposition events in this region.

571

572 At the three northern stations of the network, Le Casset (44°59'N-6°28'E), Frioul (43°15'N-5°17'E) and
573 Corsica (43°00'N-9°21'E), the maximum deposition fluxes measured on a weekly basis were 0.17 g m⁻²,
574 0.34 g m⁻² and 0.53 g m⁻², respectively. For the two southern stations, Mallorca (39°15'N-3°03'E) and
575 Lampedusa (35°31'N-12°37'E), the maximum weekly deposition fluxes are almost one order of
576 magnitude higher, 3.2 g m⁻² wk⁻¹ and 2.7 g m⁻² wk⁻¹, respectively. Deposition fluxes for 1-yr
577 measurements ranged from 7.4 g m⁻² yr⁻¹ in the southern part of the western Mediterranean to
578 0.9 g m⁻² yr⁻¹ at the French northern station. This confirms a strong South-to-North decreasing gradient of
579 the atmospheric deposition mass flux in the western Mediterranean region. These annual deposition
580 fluxes are significantly lower than those previously measured between the 1980's and early 2000's
581 mainly because only few intense deposition events (>1 g m⁻²) were recorded. These results seem to be in
582 agreement with the decreasing trend of PM10 concentrations over the Mediterranean region and with
583 variation in large scale atmospheric circulation affecting dust atmospheric contents (lower values of the
584 NAO indices during the last two decades).

585

586 We selected the 98 most intense dust deposition events (MIDD) for the investigated period. They
587 occurred preferentially in spring whatever the sampling station. However, the southern stations of the
588 network (Lampedusa and Mallorca) exhibit a second maximum in autumn while the northern stations
589 (Corsica, Frioul, Le Casset) exhibit this second maximum in summer. Few dust deposition events were
590 recorded simultaneously on several stations, suggesting that different dust events contribute to the
591 deposition measured in different parts of the western Mediterranean.

592

593 By matching satellite observations of MODIS AOD and HYSPLIT air mass trajectories, we defined 7
594 large Saharan dust provenance areas and discussed how they contribute to dust deposition in the western
595 Mediterranean region. The western Sahara is by far the most frequent dust provenance of the intense dust
596 deposition measured in the northern and western part of the western Mediterranean basin. The central and
597 the south-eastern parts of the western basin are equally affected by dust transported from western and

598 eastern Saharan regions. In the same way, we also discussed the main dust transport trajectories leading to
599 the Saharan dust deposition in the different parts of the western Mediterranean. We identified six major
600 dust transport routes. Three of them, corresponding to 70% of all trajectories, are dominant in spring (one
601 trajectory type, (a)) and in summer (the other two, (c and d)).

602

603 Finally, we showed that several dust deposition events (DDE) can contribute to high weekly dust
604 deposition fluxes measured in the stations of the network. The daily precipitation measured at the station
605 allowed us to discuss the relative contribution of wet and dry dust deposition to the weekly deposition
606 fluxes. Even if the procedure we used only allows to roughly estimating wet vs dry deposition
607 occurrences, the dry deposition can contribute significantly for the highest deposition fluxes (MIDD) to
608 the total deposition, from 10% and 46% of the total deposited mass depending on the station.

609

610 The results show that dust deposition in the western Mediterranean region is far to be homogeneous. A
611 high spatial and temporal variability of the deposition is observed. A South to North decrease of the
612 intensity of the deposition fluxes is noticed. Moreover, during the investigated period, different source
613 regions contribute to the dust deposition in different locations of the central and western Mediterranean in
614 relation with different dust transport pathways. Our results suggest a seasonal pattern of the Saharan high
615 dust deposition within the western Mediterranean basin for the investigated period, which could be
616 refined with longer time series of deposition measurements. This unique dataset will be used to test the
617 dust deposition in atmospheric transport models in complement to other aerosols measurements available
618 at the stations.

619

620

621 **Acknowledgments**

622

623 This study was funded by the PRIMEQUAL-ADEME programme on « Pollution atmosphérique longue
624 distance » through the research project « Mesure du dépôt atmosphérique et validation de sa
625 représentation dans les modèles régionaux » (DEMO project, contract n°0962c0067). This project was
626 also funded by the MISTRALS (Mediterranean Integrated Studies at Local and Regional Scales)
627 programme as part of the Chemistry Aerosol Mediterranean Experiment (ChArMEx) and by the Spanish
628 Government project ChArMEx (The Chemistry-Aerosol Mediterranean Experiment): aerosols deposition
629 Ref: CTM2011-14036-E. The development of the CARAGA collector was supported both by the
630 Chemistry Faculty of the Paris Diderot University and the PRIMEQUAL-ADEME DEMO project. The
631 authors would like to thank M.-D. Loÿe-Pilot and two anonymous reviewers for their insightful and
632 helpful comments on the manuscript. Terra-and Aqua-MODIS AOD used in this study were produced
633 with the Giovanni online data system, developed and maintained by the NASA Goddard Earth Sciences

634 (GES) Data and Information Services Center (DISC). We thank the HYSPLIT teams for making the
635 backward and forward air mass trajectories available, and EUMETSAT and ICARE for the MSG/SEVIRI
636 products.
637

638 **References**

- 639 Alfaro, S. and Gomes, L.: Modeling mineral aerosol production by wind erosion: Emission intensities and
640 aerosol distributions in source areas, *J. Geophys. Res.*, 106, 18075-18084, 2001
- 641 Avila, A., Queralt-Mitjans, I., and Alarcón, M.: Mineralogical composition of African dust delivered by
642 red rains over northeastern Spain, *J. Geophys. Res.*, 102, 21977-21996, doi:10.1029/97JD00485, 1997.
- 643 Avila, A., Alarcón, M., Castillo, S., Escudero, M., Orellana, J. G., Masqué, P., and Querol, X.: Variation
644 of soluble and insoluble calcium in red rains related to dust sources and transport patterns from North
645 Africa to northeastern Spain, *J. Geophys. Res.*, 112, 1–14, doi:10.1029/2006JD007153, 2007.
- 646 Barnaba, F., and Gobbi, G. P.: Aerosol seasonal variability over the Mediterranean region and relative
647 impact of maritime, continental and Saharan dust particles over the basin from MODIS data in the year
648 2001, *Atmos. Chem. Phys.*, 4, 2367-2391, doi:10.5194/acp-4-2367-2004, 2004
- 649 Bergametti, G., Gomes, L., Remoudaki, E., Desbois, M., Martin, D., and Buat-Ménard, P.: Present
650 transport and deposition patterns of African dusts to the north-western Mediterranean, in:
651 *Paleometeorology: Modern and Past Patterns of Global Atmospheric Transport*, edited by: Leinen, M. and
652 Sarnthein, M., Kluwer, Dordrecht, 227–252, 1989.
- 653 Bergametti, G. and Fôret, G., Dust deposition, in *Mineral Dust: A Key Player in the Earth System*, P.
654 Knippertz and J.-B.W. Stuut (eds.), 179-200, doi:10.1007/978-94-017-8978-3__8, Springer, Dordrecht,
655 2014
- 656 Brooks, N., and Legrand, M.: Dust variability over northern Africa and rainfall in the Sahel. In *Linking*
657 *Land Surface change to climate change*, edited by: McLaren, S. J. and Kniveton, D., Kluwer Academic
658 Publishers, Dordrecht, 1–25, 2000.
- 659 Cautenet, G., Guillard, F., Marticorena, B., Bergametti, G., Dulac, F. and Edy, J.: Modelling of a Saharan
660 dust event. *Meteorologische Zeitschrift*, 9, 221-230, 2000.
- 661 Chin, M., Ginoux, P., Kinne, S., Torres, O., Holben, B. N., Duncan, B. N., Martin, R. V., Logan, J. A.,
662 Higurashi, A. and Nakajima, T.: Tropospheric aerosol optical thickness from the GOCART model and
663 comparisons with satellite and Sun photometer measurements. *J. Atmos. Sci.*, 59, 461-483,
664 doi:10.1175/1520-0469(2002)059<0461:TAOTFT>2.0.CO, 2002.
- 665 di Iorio, T., di Sarra, A., Sferlazzo, D. M., Cacciani, M., Meloni, D., Monteleone, F., Fuà, D., and Fiocco
666 G.: Seasonal evolution of the tropospheric aerosol vertical profile in the central Mediterranean and role of
667 desert dust, *J. Geophys. Res.*, 114, D02201, doi:10.1029/2008JD010593, 2009.
- 668 di Sarra, A., di Iorio, T., Cacciani, M., Fiocco, G., and Fuà, D.: Saharan dust profiles measured by lidar at
669 Lampedusa, *J. Geophys. Res.*, 106, 10335, doi:10.1029/2000JD900734, 2001.
- 670 Draxler, R.R. and Rolph, G.D.: HYSPLIT (HYbrid Single-Particle Lagrangian Integrated Trajectory)
671 Model access via NOAA ARL READY Website (<https://ready.arl.noaa.gov/HYSPLIT.php/>), NOAA Air
672 Resources Laboratory, College Park, MD, 2003.
- 673 Duce, R. A. and Tindale, N. W.: Atmospheric transport of iron and its deposition in the ocean. *Limnology*
674 *and Oceanography*, 36, 1715-1726, 1991.

- 675 Escudero, M., Castillo, S., Querol, X., Avila, A., Alarcón, M., Viana, M. M., Alastuey, A., Cuevas, E.,
676 and Rodríguez, S.: Wet and dry African dust episodes over eastern Spain, *J. Geophys. Res.* 110, D18S08,
677 doi:10.1029/2004JD004731, 2005.
- 678 Escudero, M., Stein, A. F., Draxler, R. R., Querol, X., Alastuey, A., Castillo, S., and Avila, A.: Source
679 apportionment for African dust outbreaks over the Western Mediterranean using the HYSPLIT model,
680 *Atmos. Res.*, 99, 518–527, doi:10.1016/j.atmosres.2010.12.002, 2011.
- 681 Fiol, L. A., Fornós, J. J., Gelabert, B., and Guijarro, J. A.: Dust rains in Mallorca (western
682 Mediterranean): their occurrence and role in some recent geological processes, *Catena*, 63, 64–84,
683 doi:10.1016/j.catena.2005.06.012, 2005.
- 684 Ganor, E., and Foner, H. A.: Mineral dust concentrations, deposition fluxes and deposition velocities in
685 dust episodes over Israel, *J. Geophys. Res.*, 106, 18,431–18,437, doi:10.1029/2000JD900535, 2001.
- 686 Ginoux, P. and Torres, O.: Empirical TOMS index for dust aerosol: Applications to model validation and
687 source characterization. *J. Geophys. Res.*, 108, 4534, doi:10.1029/2003JD003470, 2003.
- 688 Guerzoni, S., Landuzzi, W., Lenaz, R., Quarantotto, G., Rampazzo, G., Molinaroli, E., Turetta, C., Visin,
689 F., Cesari, G., and Cristini, S.: Fluxes of soluble and insoluble metals and nutrients from the atmosphere
690 to the central Mediterranean Sea, *Water Poll. Res. Rep.*, 30, 438–493, 1993.
- 691 Guerzoni, S., Molinaroli, E., and Chester, R.: Saharan dust inputs to the western Mediterranean Sea:
692 Depositional patterns, geochemistry and sedimentological implications, *Deep. Res. Part II Top. Stud.*
693 *Oceanogr.*, 44, 631–654, doi:10.1016/S0967-0645(96)00096-3, 1997.
- 694 Guerzoni, S., Molinaroli, E., Rossini, P., Rampazzo, G., Quarantotto, G., De Falco, G., and Cristini, S.:
695 Role of desert aerosol in metal fluxes in the Mediterranean area, *Chemosphere*, 39, 229–246,
696 doi:10.1016/S0045-6535(99)00105-8, 1999.
- 697 Guieu, C., Loÿe-Pilot, M. D., Ridame, C., and Thomas, C.: Chemical characterization of the Saharan dust
698 end-member: Some biogeochemical implications for the western Mediterranean Sea, *J. Geophys. Res.*,
699 107, 4258, doi:10.1029/2001JD000582, 2002.
- 700 Guieu, C., Loÿe-Pilot, M. D., Benyahya, L., and Dufour, A.: Spatial variability of atmospheric fluxes of
701 metals (Al, Fe, Cd, Zn and Pb) and phosphorus over the whole Mediterranean from a one-year monitoring
702 experiment: Biogeochemical implications, *Mar. Chem.*, 120, 164–178,
703 doi:10.1016/j.marchem.2009.02.004, 2010.
- 704 Hamonou, E., Chazette, P., Balis, D., Dulac, F., Schneider, X., Galani, E., Ancellet, G., and Papayannis,
705 A.: Characterization of the vertical structure of Saharan dust export to the Mediterranean basin, *J.*
706 *Geophys. Res.*, 104, 22257–22270, doi:10.1029/1999JD900257, 1999.
- 707 Holben, B. N., Smirnov, A., Eck, T. F., Slutsker, I., Abuhassan, N., Newcomb, W. W., Schafer, J. S.,
708 Chatenet, B., Lavenu, F., Kaufman, Y. J., Vande Castle, J., Setzer, A., Markham, B., Clark, D., Frouin,
709 R., Halthore, R., Karneli, A., O’Neill, N. T., Pietras, C., Pinker, R. T., Voss, K., and Zibordi, G.: An
710 emerging ground-based aerosol climatology- Aerosol optical depth from AERONET. *J. Geophys. Res.*,
711 106, 12067–12097, 2001.
- 712 Huneus, N., Schulz, M., Balkanski, Y., Griesfeller, J., Prospero, J., Kinne, S., Bauer, S., Boucher, O.,
713 Chin, M., Dentener, F., Diehl, T., Easter, R., Fillmore, D., Ghan, S., Ginoux, P., Grini, A., Horowitz, L.,
714 Koch, D., Krol, M. C., Landing, W., Liu, X., Mahowald, N., Miller, R., Morcrette, J. J., Myhre, G.,
715 Penner, J., Perlwitz, J., Stier, P., Takemura, T., and Zender, C. S.: Global dust model intercomparison in
716 AeroCom phase I, *Atmos. Chem. Phys.*, 11, 7781–7816, doi:10.5194/acp-11-7781-2011, 2011.

- 717 Israelevich, P. L., Levin, Z., Joseph, J. H., and Ganor, E.: Desert aerosol transport in the Mediterranean
718 region as inferred from the TOMS aerosol index, *J. Geophys. Res. Atmos.*, 107, 1–13,
719 doi:10.1029/2001JD002011, 2002.
- 720 Israelevich, P. L.: Annual variations of physical properties of desert dust over Israel, *J. Geophys. Res.*,
721 108, 1–9, doi:10.1029/2002JD003163, 2003.
- 722 Jorba, O., Pérez, C., Rocadenbosch, F., and Baldasano, J.: Cluster Analysis of 4-Day Back Trajectories
723 Arriving in the Barcelona Area, Spain, from 1997 to 2002, *J. Appl. Meteorol.*, 43, 887–901,
724 doi:10.1175/1520-0450(2004)043<0887:CAODBT>2.0.CO, 2004.
- 725 Kubilay, N., Nickovic, S., Moulin, C., and Dulac, F.: An illustration of the transport and deposition of
726 mineral dust onto the eastern Mediterranean, *Atmos. Environ.*, 34, 1293–1303, doi:10.1016/S1352-
727 2310(99)00179-X, 2000.
- 728 Laurent, B., Losno, R., Chevaillier, S., Vincent, J., Rouillet, P., Bon Nguyen, E., Ouboulmane N., Triquet
729 S., Fournier M., Raimbault P., and Bergametti G.: An automatic collector to monitor insoluble atmospheric
730 deposition: an application for mineral dust deposition. *Atmos. Meas. Tech.*, 8, 2801–2811,
731 doi:10.5194/amt-8-2801-2015, 2015.
- 732 Le Bolloch, O., Guerzoni, S. and Molinaroli, E.: Atmosphere-Ocean mass fluxes at two coastal sites in
733 Sardinia (39–41° N, 8–10°E), in *The Impact of Desert Dust across the Mediterranean*, Guerzoni, S., and
734 Chester, R. Eds., Kluwer Academic Publishers, Dordrecht, 217–222, 1996.
- 735 Levy, R. C., Mattoo, S., Munchak, L. A., Remer, L. A., Sayer, A. M., Patadia, F., and Hsu, N. C.: The
736 Collection 6 MODIS aerosol products over land and ocean, *Atmos. Meas. Tech.*, 6, 2989–3034,
737 doi:10.5194/amt-6-2989-2013, 2013.
- 738 Loÿe-Pilot, M.D., Martin, J.M., and Morelli, J.: Influence of Saharan dust on the rain acidity and
739 atmospheric input to the Mediterranean, *Nature*, 321, 427–428, doi:10.1038/321427a0, 1986.
- 740 Loÿe-Pilot, M.D., and Martin, J.M.: Saharan dust input to the western Mediterranean: An eleven years
741 records in Corsica, in *The Impact of Desert Dust across the Mediterranean*, Guerzoni, S., and Chester, R.
742 Eds., Kluwer Academic Publishers, Dordrecht, 191–199, 1996.
- 743 Marconi, M., Sferlazzo, D. M., Becagli, S., Bommarito, C., Calzolari, G., Chiari, M., di Sarra, A.,
744 Ghedini, C., Gómez-Amo, J. L., Lucarelli, F., Meloni, D., Monteleone, F., Nava, S., Pace, G., Piacentino,
745 S., Rugi, F., Severi, M., Traversi, R., and Udisti, R.: Saharan dust aerosol over the central Mediterranean
746 Sea: PM10 chemical composition and concentration versus optical columnar measurements, *Atmos.*
747 *Chem. Phys.*, 14, 2039–2054, doi:10.5194/acp-14-2039-2014, 2014.
- 748 Marticorena, B., and Bergametti, G.: Modeling the atmospheric dust cycle: 1. Design of a soil-derived
749 dust production scheme, *J. Geophys. Res.*, 100, 16415–16430, 1995.
- 750 Marticorena, B., Dust production mechanisms, in *Mineral Dust: A Key Player in the Earth System*, P.
751 Knippertz and J.-B.W. Stuut (eds.), 93–120, doi:10.1007/978-94-017-8978-3__8, Springer, Dordrecht,
752 2014.
- 753 Martin, D., Bergametti, G., and Strauss, B.: On the use of the synoptic vertical velocity in trajectory
754 model: validation by geochemical tracers, *Atmos. Environ.*, 24A, 2059–2069, doi:10.1016/0960-
755 1686(90)90240-N, 1990.
- 756 Mattson, J. O., and Nihlén, T.: The transport of Saharan dust to southern Europe: a scenario, *J. Arid*
757 *Environ.*, 32, 111–119, doi:10.1006/jare.1996.0011, 1994.

- 758 Meloni, D., di Sarra, A., di Iorio, T., and Fiocco, G.: Direct radiative forcing of Saharan dust in the
759 Mediterranean from measurements at Lampedusa Island and MISR space-borne observations, *J. Geophys.*
760 *Res. D Atmos.*, 109, 1–15, doi:10.1029/2003JD003960, 2004.
- 761 Meloni, D., di Sarra, A., Monteleone, F., Pace, G., Piacentino, S., and Sferlazzo, D. M.: Seasonal
762 transport patterns of intense Saharan dust events at the Mediterranean island of Lampedusa, *Atmos. Res.*,
763 88, 134-148, doi:10.1016/j.atmosres.2007.10.007, 2008.
- 764 Morales-Baquero, R., Pulido-Villena, E., and Reche, I.: Atmospheric inputs of phosphorus and nitrogen
765 to the southwest Mediterranean region: Biogeochemical responses of high mountain lakes, *Limnol.*
766 *Oceanogr.*, 51, 830–837, doi:10.4319/lo.2006.51.2.0830, 2006.
- 767 Moulin, C., Lambert, C. E., Dulac, F., and Dayan, U.: Control of atmospheric export of dust from North
768 Africa by the North Atlantic Oscillation, *Nature*, 387, 691–694, doi:10.1038/42679, 1997.
- 769 Moulin, C., Lambert, C. E., Dayan, U., Masson, V., Ramonet, M., Bousquet, P., Legrand, M., Balkanski,
770 Y. J., Guelle, W., Marticorena, B., Bergametti, G., and Dulac, F.: Satellite climatology of African dust
771 transport in the Mediterranean atmosphere, *J. Geophys. Res.*, 103, 13137, doi:10.1029/98JD00171, 1998.
- 772 Nabat, P., Somot, S., Mallet, M., Chiapello, I., Morcrette, J. J., Solmon, F., Szopa, S., Dulac, F., Collins,
773 W., Ghan, S., Horowitz, L.W., Lamarque, J. F., Lee, Y.H., Naik, V., Nagashima, T., Shindell, D. and
774 Skeie, R.: A 4-D climatology (1979–2009) of the monthly tropospheric aerosol optical depth distribution
775 over the Mediterranean region from a comparative evaluation and blending of remote sensing and model
776 products. *Atmos. Meas. Tech.*, 6, 1287-1314, doi:10.5194/amt-6-1287-2013, 2013.
- 777 O’Hara, S. L., Clarke, M. L., and Elatrash, M. S.: Field measurements of desert dust deposition in Libya,
778 *Atmos. Environ.*, 40, 3881–3897, doi:10.1016/j.atmosenv.2006.02.020, 2006.
- 779 Pey, J., Querol, X., Alastuey, A., Forastiere, F., and Stafoggia, M.: African dust outbreaks over the
780 Mediterranean Basin during 2001-2011: PM10 concentrations, phenomenology and trends, and its
781 relation with synoptic and mesoscale meteorology, *Atmos. Chem. Phys.*, 13, 1395–1410,
782 doi:10.5194/acp-13-1395-2013, 2013.
- 783 Pongkiatkul, P., and Kim Oanh, N. T.: Assessment of potential long-range transport of particulate air
784 pollution using trajectory modeling and monitoring data, *Atmos. Res.*, 85, 3–17,
785 doi:10.1016/j.atmosres.2006.10.003, 2007.
- 786 Prospero, J. M.: Long-term measurements of the transport of African mineral dust to the southeastern
787 United States: Implications for regional air quality, *J. Geophys. Res.*, 104, 15917-15927, doi:
788 10.1029/1999JD900072, 1999.
- 789 Prospero, J. M., Ginoux, P., Torres, O., Nicholson, S. E. and Gill, T. E.: Environmental characterization
790 of global sources of atmospheric soil dust identified with the Nimbus 7 Total Ozone Mapping
791 Spectrometer (TOMS) absorbing aerosol product. *Reviews of geophysics*, 40(1), 2-1, 2002.
- 792 Pye, K.: Aeolian dust transport and deposition over Crete and adjacent parts of the Mediterranean Sea,
793 *Earth Surf. Proc. Landforms*, 17, 271-288, 1992.
- 794 Querol, X., Pey, J., Pandolfi, M., Alastuey, A., Cusack, M., Pérez, N., Moreno, N., Viana, M.,
795 Mihalopoulos, N., Kallos, G., and Kleanthous, S.: African dust contributions to mean ambient PM10
796 mass-levels across the Mediterranean basin, *Atmos. Environ.*, 43, 4266–4277, 2009.

- 797 Remer, L. A., Kleidman, R. G., Levy, R. C., Kaufman, Y. J., Tanré, D., Mattoo, S., Martins, J. V.,
798 Ichoku, C., Koren, I., Yu, H. and Holben, B. N.: Global aerosol climatology from the MODIS satellite
799 sensors. *J. Geophys. Res.*, 113, D14S07, doi:10.1029/2007JD009661, 2008.
- 800 Remoudaki, E.: Etude des processus contrôlant la variabilité temporelle des flux atmosphériques de
801 polluants et de poussières minérales en Méditerranée occidentale, Thèse de doctorat, Univ. Paris 7,
802 244 pp, 1990.
- 803 Ridame, C., Guieu, C., and Lojze-Pilot, M.-D.: Trend in total atmospheric fluxes of aluminium, iron and
804 trace metals in the northwestern Mediterranean over the past decade (1985-1997), *J. Geophys. Res.*, 104,
805 30127-30138, doi:10.1029/1999JD900747, 1999.
- 806 Salvador, P., Alonso-Pérez, S., Pey, J., Artñano, B., de Bustos, J. J., Alastuey, A., and Querol, X.:
807 African dust outbreaks over the western Mediterranean Basin: 11-year characterization of atmospheric
808 circulation patterns and dust source areas, *Atmos. Chem. Phys.*, 14, 6759-6775, doi:10.5194/acp-14-
809 6759-2014, 2014.
- 810 Scheifinger, H. and Kaiser, A.: Validation of trajectory statistical methods, *Atmos. Environ.*, 41, 8846–
811 8856, 2007.
- 812 Schepanski, K., Tegen, I., Laurent, B., Heinold, B., and Macke, A.: A new Saharan dust source activation
813 frequency map derived from MSG-SEVIRI IR-channels, *Geophys. Res. Lett.*, 34, 1–5,
814 doi:10.1029/2007GL030168, 2007.
- 815 Schepanski, K., Tegen, I., and Macke, A., Comparison of satellite based observations of Saharan dust
816 source areas, *Remote Sensing of Environment*, 123, 90-97, 2012.
- 817 Schulz, M., Prospero, J. M., Baker, A. R., Dentener, F., Ickes, L., Liss, P. S., Mahowald, N., Nickovic, S.,
818 Perez García-Pando, C., Rodríguez, S., Manmohan Sarin, O., Tegen, I., and Duce, R. A.: Atmospheric
819 transport and deposition of mineral dust to the ocean: implications for research needs. *Environmental
820 science & technology*, 46(19), 10390-10404, 2012.
- 821 Shao, Y., Raupach, M. R. and Findlater, P. A.: Effect of saltation bombardment on the entrainment of
822 dust by wind. *J. Geophys. Res.*, 98, 12719-12726, 1993.
- 823 Shao, Y.: Simplification of a dust emission scheme and comparison with data, *J. Geophys. Res.*, 109,
824 D10202, doi:10.1029/2003JD004372, 2004.
- 825 Shi, T., and Cressie, N.: Global statistical analysis of MISR aerosol data: a massive data product from
826 NASA's Terra satellite. *Environmetrics*, 18, 665-680, 2007.
- 827 Sciare, J., Oikonomou, K., Cachier, H., Mihalopoulos, N., Andreae, M.O., Maenhaut, W., and Sarda-
828 Estève, R.: Aerosol mass closure and reconstruction of the light scattering coefficient over the Eastern
829 Mediterranean Sea during the MINOS campaign, *Atmos. Chem. Phys.*, 5, 2253-2265, 2005.
- 830 Sheldon, R. W.: Size separation of marine seston by membrane and glass-fiber filters, *Limnol. Oceanogr.*,
831 17, 494–498, 1972.
- 832 Smirnov, A., Holben, B. N., Giles, D. M., Slutsker, I., O'Neill, N. T., Eck, T. F., Macke, A., Croot, P.,
833 Courcoux, Y., Sakerin, S. M., Smyth, T. J., Zielinski, T., Zibordi, G., Goes, J. I., Harvey, M. J., Quinn, P.
834 K., Nelson, N. B., Radionov, V. F., Duarte, C. M., Losno, R., Sciare, J., Voss, K. J., Kinne, S., Nalli, N.
835 R., Joseph, E., Krishna Moorthy, K., Covert, D. S., Gulev, S. K., Milinevsky, G., Larouche, P., Belanger,
836 S., Horne, E., Chin, M., Remer, L. A., Kahn, R. A., Reid, J. S., Schulz, M., Heald, C. L., Zhang, J.,

- 837 Lapina, K., Kleidman, R. G., Griesfeller, J., Gaitley, B. J., Tan, Q. and Diehl, T. L.: Maritime Aerosol
838 Network as a component of AERONET-first results and comparison with global aerosol models and
839 satellite retrievals. *Atmos. Meas. Tech. Discuss.*, 4, 1-32, doi:10.5194/amtd-4-1-2011, 2011.
- 840 Stohl, A.: Computation, accuracy and applications of trajectories – a review and bibliography, *Atmos.*
841 *Environ.*, 32, 947–966, 1998.
- 842 TERNON, E., Guieu, C., Loÿe-Pilot, M. D., Leblond, N., Bosc, E., Gasser, B., Miquel, J.C., and Martin, J.:
843 The impact of Saharan dust on the particulate export in the water column of the North Western
844 Mediterranean Sea, *Biogeosci.*, 7, 809-826, doi:10.5194/bg-7-809-2010, 2010.
- 845 Textor, C., Schulz, M., Guibert, S., Kinne, S., Balkanski, Y., Bauer, S., Berntsen, T., Berglen, T.,
846 Boucher, O., Chin, M., Dentener, F., Diehl, T., Easter, R., Feichter, H., Fillmore, D., Ghan, S., Ginoux,
847 P., Gong, S., Grini, A., Hendricks, J., Horowitz, L., Huang, P., Isaksen, I., Iversen, I., Kloster, S., Koch,
848 D., Kirkevåg, A., Kristjansson, J. E., Krol, M., Lauer, A., Lamarque, J. F., Liu, X., Montanaro, V.,
849 Myhre, G., Penner, J., Pitari, G., Reddy, S., Seland, Ø., Stier, P., Takemura, T. and Tie, X.: Analysis and
850 quantification of the diversities of aerosol life cycles within AeroCom. *Atmospheric Chemistry and*
851 *Physics*, 6, 1777-1813, 2006.
- 852 Torres, O., Bhartia, P. K., Herman, J. R., Sinyuk, A., Ginoux, P., and Holben, B.: A long-term record of
853 aerosol optical depth from TOMS observations and comparison to AERONET measurements, *J. Atmos.*
854 *Sci.*, 59, 398-413, 2002.
- 855 Usero, J., and Gracia, I.: Trace and major elements in atmospheric deposition in the “Campo de Gibraltar”
856 region, *Atmos. Environ.*, 20, 1639–1646, doi:10.1016/0004-6981(86)90254-4, 1986.
- 857 Washington, R., Todd, M., Middleton, N. J., and Goudie, A. S.: Dust-storm source areas determined by
858 the total ozone monitoring spectrometer and surface observations. *Annals of the Association of American*
859 *Geographers*, 93, 297-313, 2003.
- 860 Zender, C. S., Miller, R. L. R. L., and Tegen, I.: Quantifying mineral dust mass budgets: Terminology,
861 constraints, and current estimates. *Eos, Transactions American Geophysical Union*, 85, 509-512, 2004.
- 862
863

864 Table 1: Dust deposition fluxes measured in the Mediterranean basin and Northern Africa. (*) Sampling
 865 performed in different places and periods, (**) in different places, (~) assuming Al is 7.1% of total dust
 866 (Guieu et al., 2002).

Region	Location	Period	Duration	Deposition flux (g m ⁻² yr ⁻¹)	Comments	Reference
Western Mediterranean	Cap Ferrat and 3 sites SE France and NW Corsica	2003–2007	4 years (*)	11.4	Insoluble	Ternon et al. (2010)
	Cap Bear, SW France	2001–2002	12 months	10.6 (~)	Bulk	Guieu et al. (2010)
	Capo Cavallo, NW Corsica	1985–1986	12.5 months	12.5 (~)	Bulk	Bergametti et al. (1989)
		1986–1987	20 months	9.7	Bulk	Remoudaki (1990)
	3 inland sites, Corsica Isl.	1984–1994		4–26	Bulk	Loÿe-Pilot and Martin (1996)
	Ostriconi, N Corsica	2001–2002	12 months	27.4 (~)	Bulk	Guieu et al. (2010)
	Pirio, NW Corsica	1995–1997	27 months	2–4 (~)	Bulk	Ridame et al. 1999
		1999–2000	13 months (*)	9–14 (~)	Bulk	Loÿe-Pilot et al. 2001
	Capo Carbonara, SE Sardinia	1990–1992	19 months	12.8 (~)	Bulk	Guerzoni et al. (1999)
	Montseny, NE Spain	1983–1994	11 years	5.2 Dust rains only	Bulk	Avila et al. (1997)
	Palma de , Balears	1982–2003	22 years	~14 Dust rains only	Bulk	Fiol et al. (2005)
Campo de Gibraltar S Spain	1982–1983	12 months	22.8 (~)	Soluble + Insoluble	Usero and Gracia (1986)	
Lanjaron, SE Spain	2001–2002	23 months	11.1	Bulk	Morales-Baquero et al. (2006)	
Eastern Mediterranean	Erdemli, SE Turkey	1991–1992	16 months	13.0	Bulk	Kubilay et al. (2000)
	Akkuyu, SE Turkey	2001–2002	12 months	10.1 (~)	Bulk	Guieu et al. (2010)
	6 sites, Crete	1988–1994	6 years	11–23	Bulk	Mattson and Nihlén (1994)
	7 sites, Crete	1988–1990	34 month	10–100	Bulk	Pye (1992)
	Finokalia, NE Crete	2001–2002	12 months	8.8 (~)	Bulk	Guieu et al. (2010)
	Cavo Greco, SE Cyprus	2001–2002	12 months	4.2 (~)	Bulk	Guieu et al. (2010)
	Mytilene, Lesbos Isl.	2001–2002	12 months	5.4 (~)	Bulk	Guieu et al. (2010)
Israel	1965 – 1995	(*)	30 – 90	Insoluble	Ganor and Foner (2001)	
North Africa	Alexandria, N. Egypt	2001–2002	8.5 months	20.3 (~)	Bulk	Guieu et al. (2010)
	14 inland sites, N. Libya	2000–2001	12 months	58 (< 20 µm only)	Bulk	O’Hara et al. (2006)
	Cap Spartel, N Morocco	2001–2002	12 months	7.2 (~)	Bulk	Guieu et al. (2010)

	Mahdia, E Tunisia	2001–2002	12 months	23.3 (~)	Bulk	Guieu et al. (2010)
--	----------------------	-----------	-----------	----------	------	---------------------

867

869 Table 2: Number of weekly deposition fluxes measured, number (and relative proportion in %) of the
 870 most intense weekly deposition fluxes recorded (MID), number of MID events with identified Saharan
 871 provenance area (MIDD), and their respective contribution (% in mass) to the deposition fluxes
 872 measured, at each station of the network.

	Number of weekly samples	Total deposition flux (g m ⁻² yr ⁻¹)	Threshold flux (g m ⁻² wk ⁻¹)	MID	MID contribution to total deposition fluxes (%)	MIDD	MIDD contribution to total deposition fluxes (%)
Le Casset	119	2.17	0.036	18 (15%)	61	15	53
Frioul	123	5.84	0.093	21 (17%)	55	18	49
Corsica	78	2.59	0.050	11 (14%)	73	11	73
Mallorca	117	9.74	0.093	21 (18%)	80	20	78
Lampedusa	100	16.0	0.093	37 (37%)	87	34	84

873

874

875

876 Table 3: Number of stations operating and number of stations recording a MIDD during the same
877 sampling week.

		Number of stations recording simultaneously a MIDD					Total
		5	4	3	2	1	
Number of stations operating	5	0	1	0	3	23	27
	4	-	0	4	7	23	35
	3	-	-	0	0	7	4
	2	-	-	-	2	2	6
	1	-	-	-	-	3	3
Total		0	1	4	12	58	75

878

879

881 Table 4: MIDD during which DDE occur only by dry, by wet or by mixed (wet + dry) deposition. The
 882 wet (or dry) conditions are defined considering the precipitation occurrence (or not) during the 24 h
 883 before the arrival time of a dust plume at the sampling sites according to the air-mass trajectories and 24,
 884 48 and 72 h after its arrival time. * Precipitation data was not available for one MIDD at the Frioul
 885 station.

886

	Time period after dust arrival	Number of MIDD				MIDD cumulated mass			
		Total	Wet deposition	Dry deposition	Wet + dry deposition (mixed)	Total mass (g m ⁻²)	Wet deposition (%)	Dry deposition (%)	Wet + dry deposition (mixed, %)
Le Casset	24h	15	12	3	-	1.2	77	23	-
	48h		13	1	1		82	14	4
	72h		13	1	1		82	14	4
Frioul	24h	17*	10	6	1	2.7	61	27	12
	48h		11	5	1		66	22	12
	72h		11	5	1		66	22	12
Corsica	24h	11	7	3	1	1.9	69	15	16
	48h		7	3	1		69	15	16
	72h		8	2	1		74	10	16
Mallorca	24h	20	12	6	2	7.6	36	15	49
	48h		14	4	2		41	10	49
	72h		14	4	2		41	10	49
Lampedusa	24h	34	18	15	1	13.5	51	46	3
	48h		18	15	1		51	46	3
	72h		18	15	1		51	46	3

887

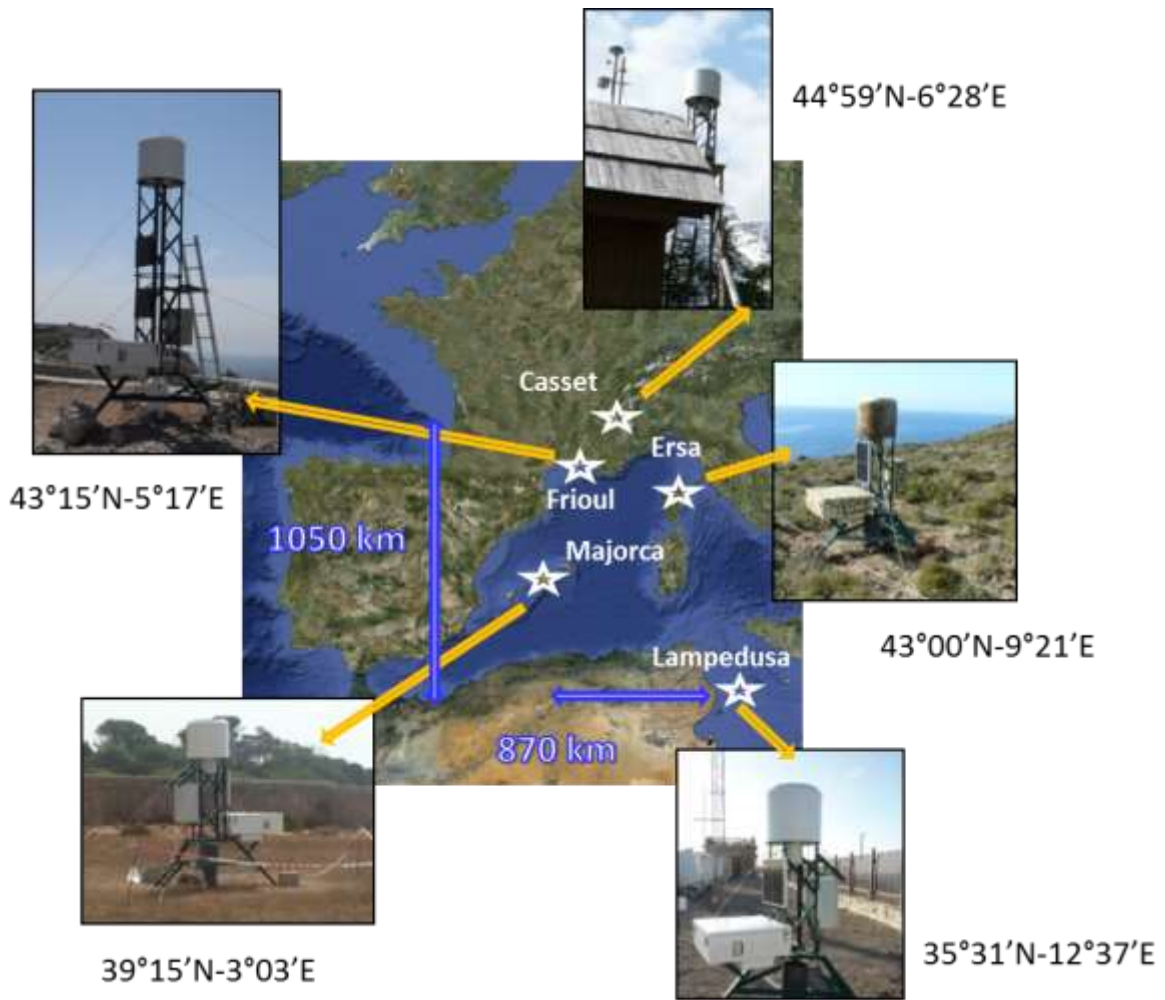
888



889

890 Figure 1: The CARAGA collector operating on Frioul Island.

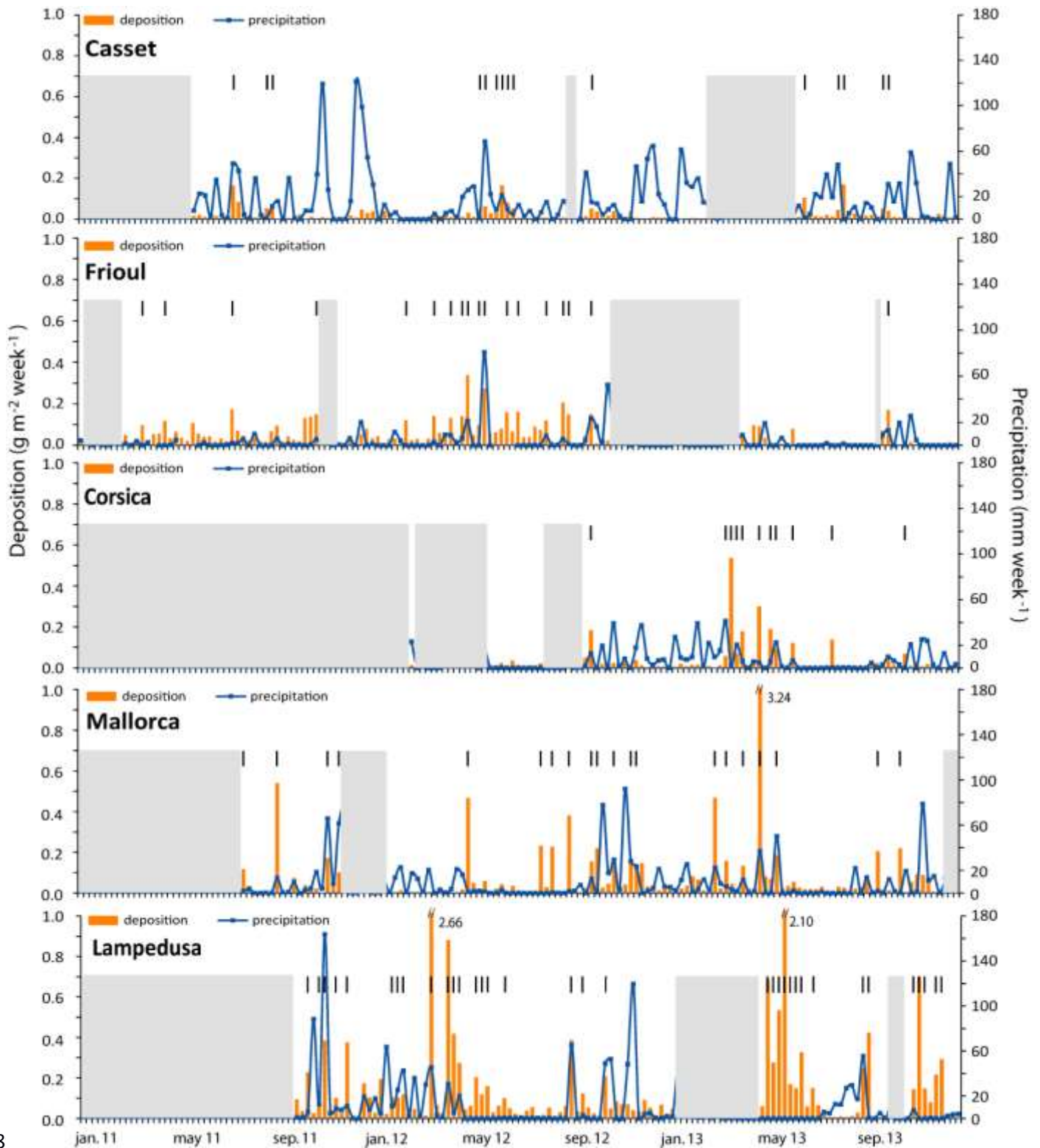
891



893

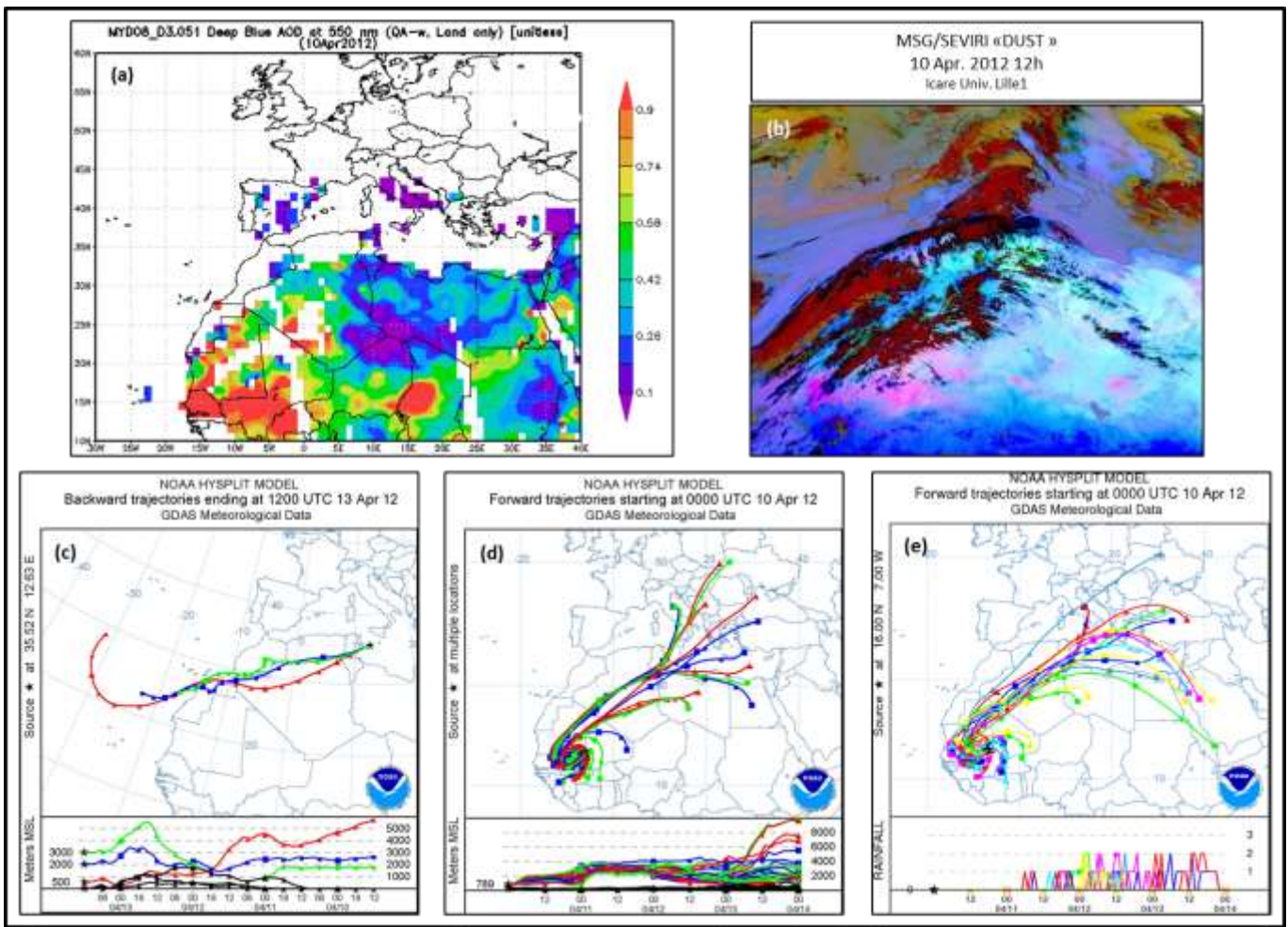
894 Figure 2: Location of the CARAGA samplers constituting the deposition network deployed in the western
 895 Mediterranean basin and southern of France.

896



8

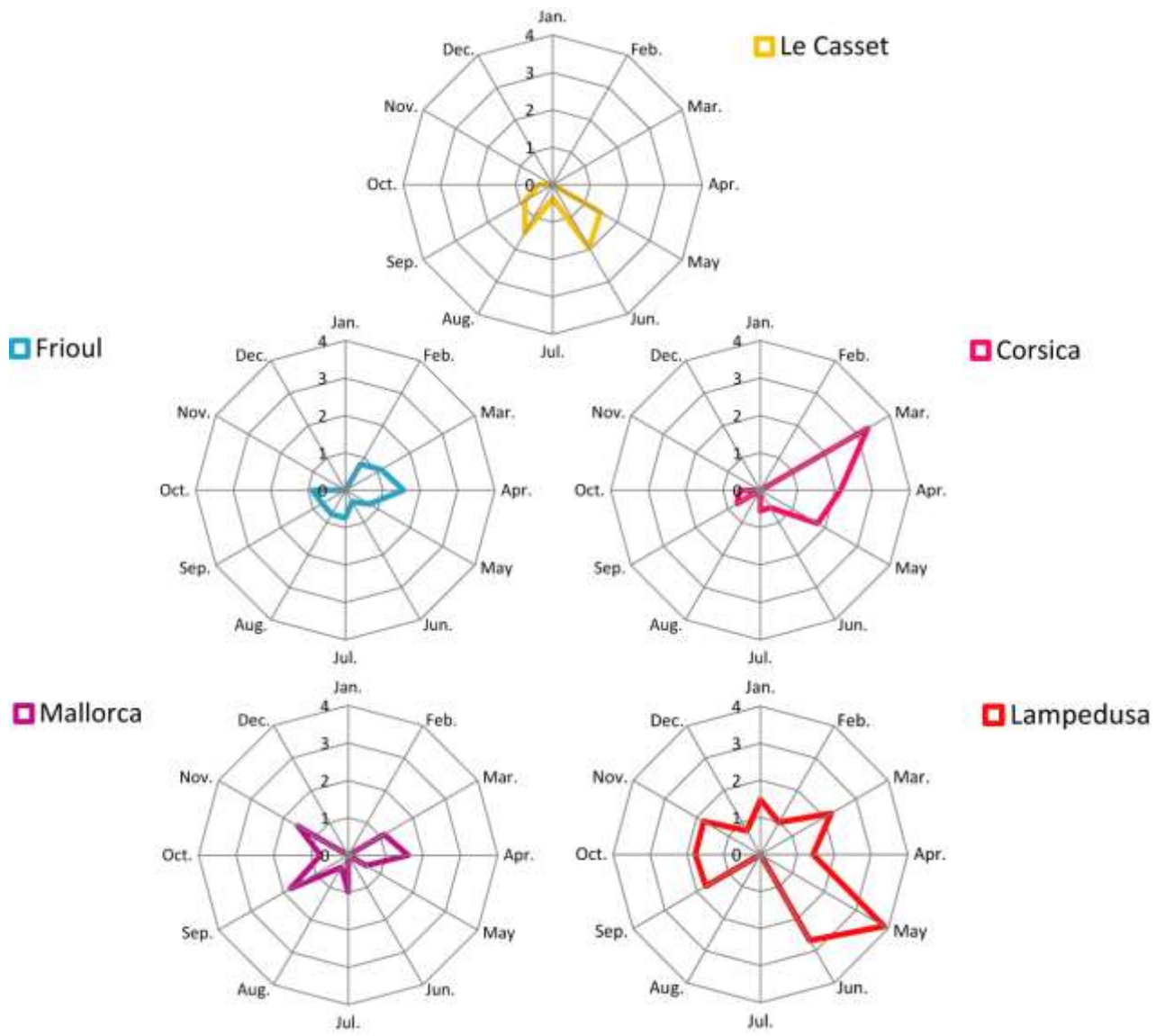
899 Figure 3: Weekly insoluble mineral deposition fluxes (orange bars) and precipitation amount (blue line)
 900 for Lampedusa, Mallorca, Corsica, Frioul and Le Casset from January 2011 to December 2013. The grey
 901 areas correspond to periods without sampling. The numbers of most intense dust deposition for each
 902 station as described in §4.3 are indicated by black bars above the deposition flux values: 34 in
 903 Lampedusa, 20 in Mallorca, 11 in Corsica, 18 in Frioul and 15 in Le Casset.



905

906 Figure 4: Illustration of the data used jointly to identify a dust transport event and its origin which leads to
 907 high deposition in Lampedusa between April 12 and 13 2012. (a) MODIS deep blue AOD, (b)
 908 MSG/SEVIRI dust false-colour composite product, (c) HYSPLIT backward trajectories for 3 starting
 909 heights (500, 2000 and 3000 m), (d) HYSPLIT forward trajectories in matrix mode with corresponding
 910 altitudes, (e) HYSPLIT forward trajectories in ensemble mode with corresponding precipitation.

911

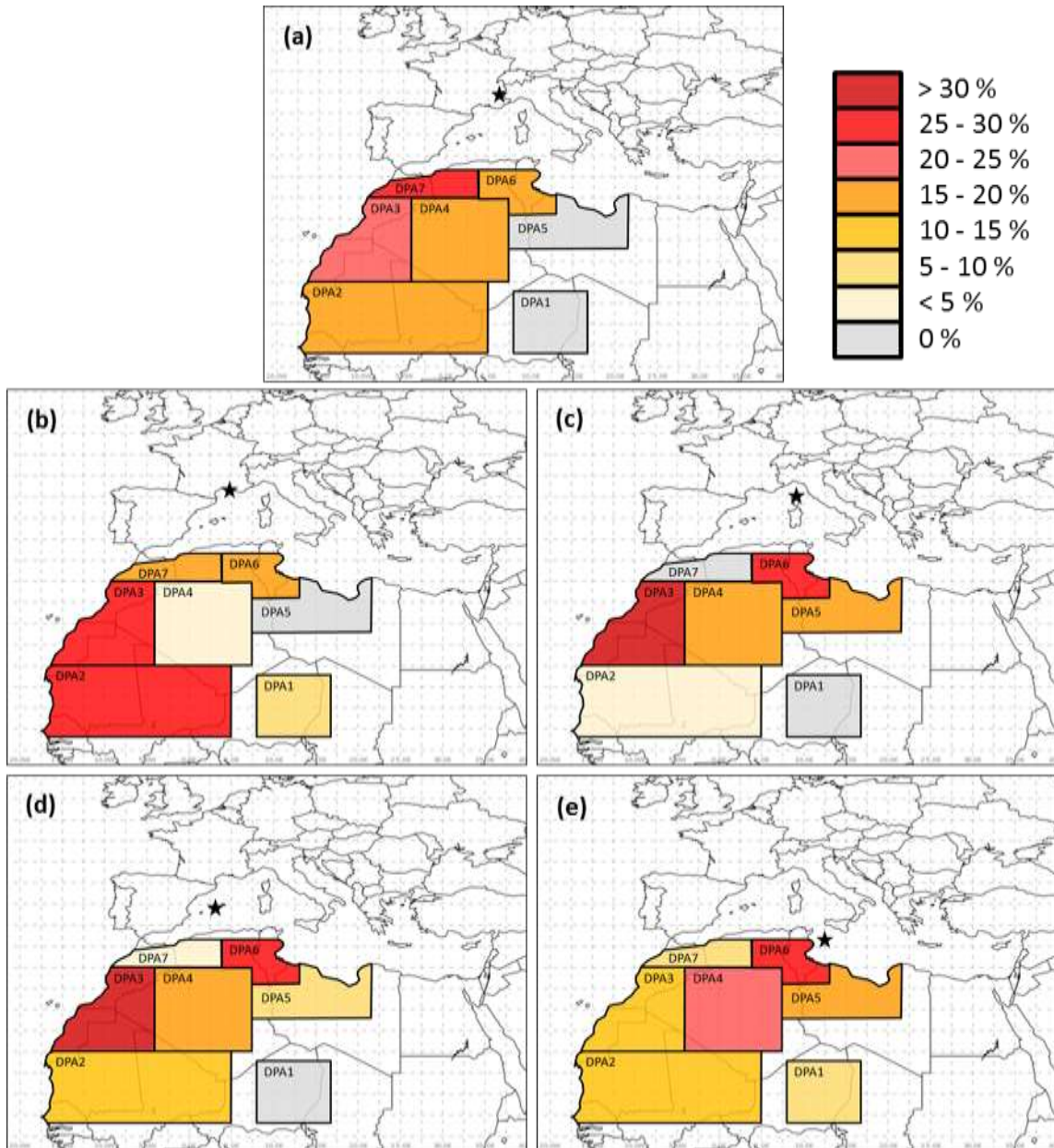


913

914 Figure 5: Weighted number of occurrence of MIDD per month over the whole sampling period at each
915 site.

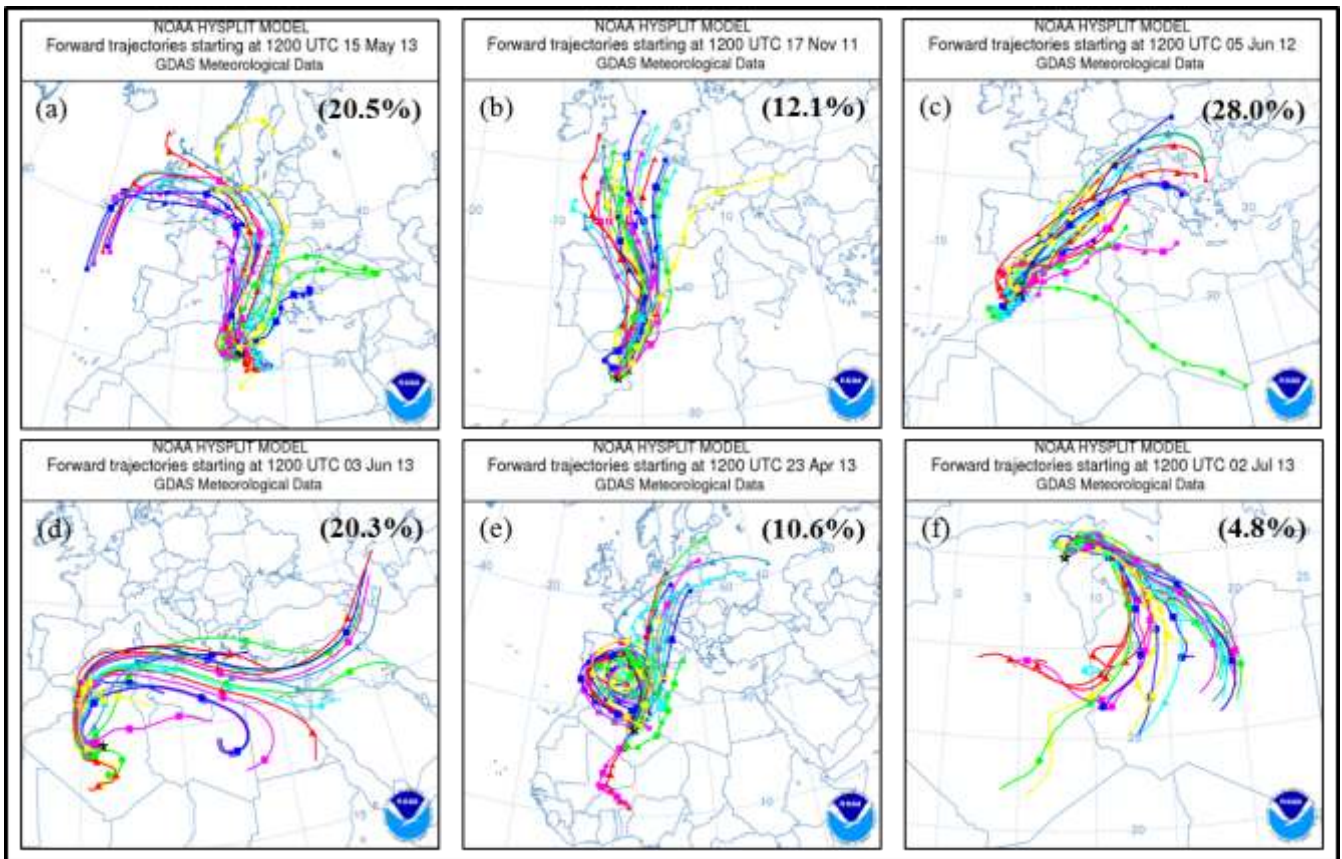
916

917
918



919
920
921
922
923

Figure 6: Frequency of dust provenance areas identified using MODIS AOD and HYSPLIT air mass trajectories for the DDE contributing to the MIDD recorded at (a) Le Casset, (b) Frioul, (c) Corsica, (d) Mallorca, and (e) Lampedusa.

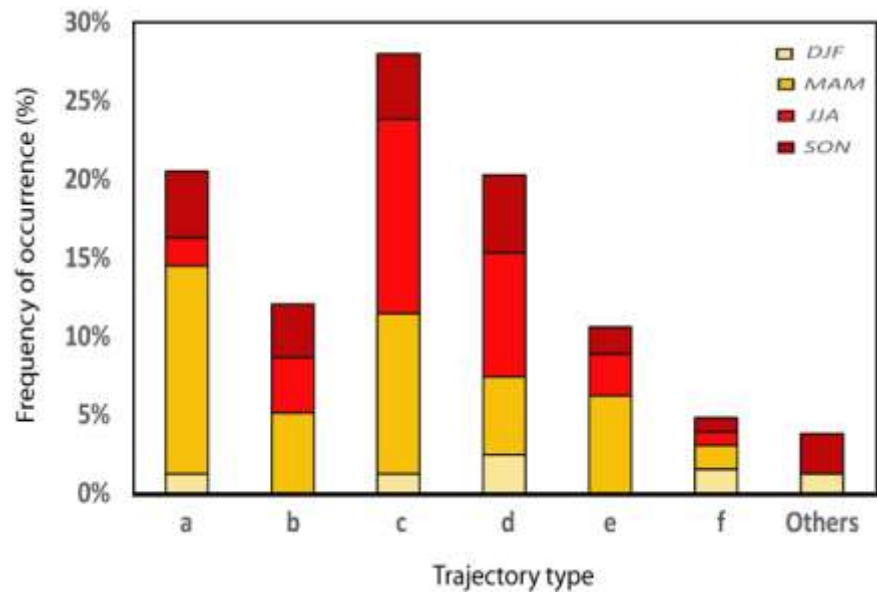


925

926 Figure 7: Typical forward air-mass trajectories computed with the HYSPLIT model and corresponding to
 927 the different Saharan deposition events collected over the western Mediterranean basin. The number in
 928 brackets indicates the relative occurrence frequency for each of the six cases (3.7% are unclassified).

929

930

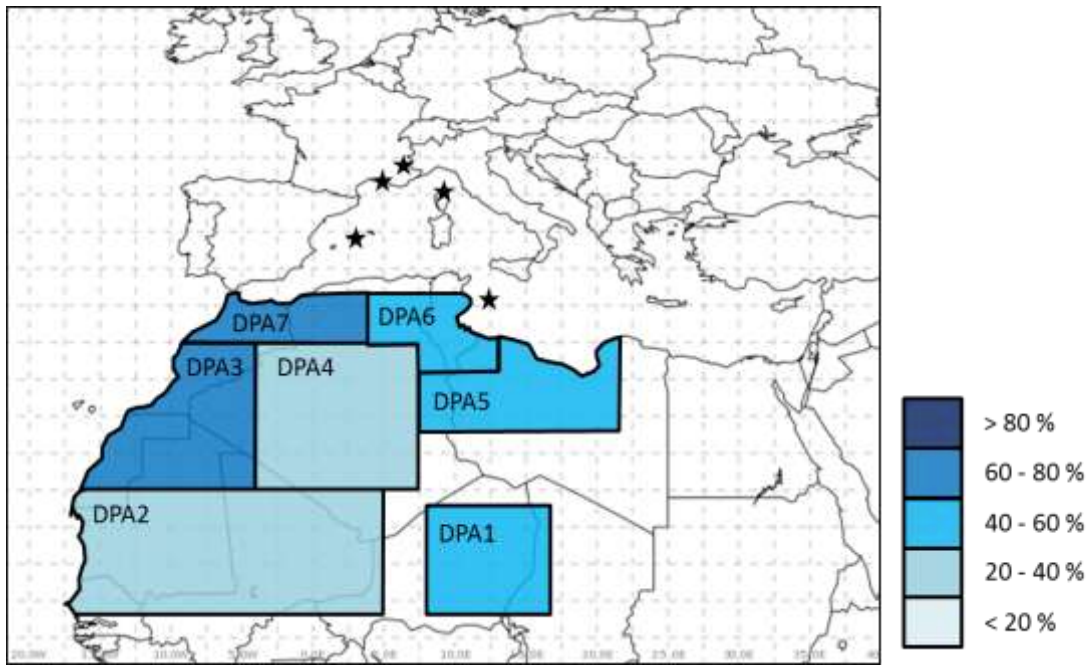


931

932 Figure 8: Seasonal occurrence of the different Saharan dust trajectories (see text for details).

933

934



935

936 Figure 9: Proportion of HYSPLIT trajectories for the DDE (in %) with precipitation during their transport
937 between the source-regions and the western Mediterranean basin.

938

939